STUDY OF RO SYSTEM FOR ITS PERFORMANCE ON VARIOUS MEMBRANES

A DISSERTATION

Submitted in partial fulfilment of the
requirements for the award of the degree
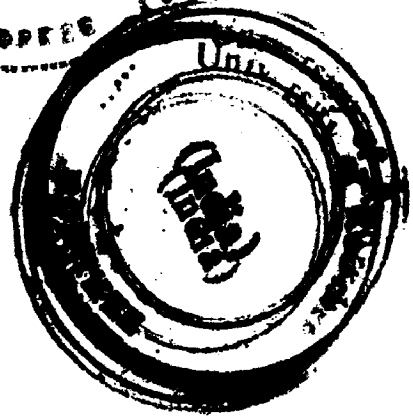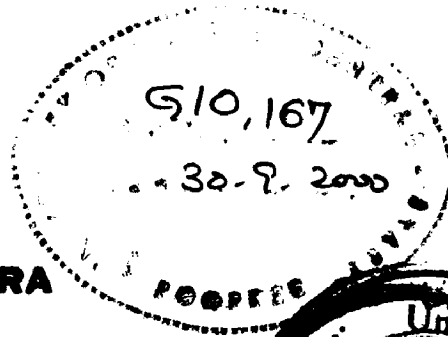*of*
MASTER OF ENGINEERING
in
CHEMICAL ENGINEERING
(With Specialization in Computer Aided Process Plant Design)

By

CHITRA

DEPARTMENT OF CHEMICAL ENGINEERING
UNIVERSITY OF ROORKEE
ROORKEE-247 667 (INDIA)

MARCH, 2000

CANDIDATE'S DECLARATION

I hereby certify that the work which is being presented in the dissertation entitled "STUDY OF RO SYSTEM FOR ITS PERFORMANCE ON VARIOUS MEMBRANES", in partial fulfilment of the requirement for the award of the degree of *MASTER OF ENGINEERING IN CHEMICAL ENGINEERING WITH SPECIALIZATION IN COMPUTER AIDED PROCESS PLANT DESIGN*, submitted in the Department of Chemical Engineering, University of Roorkee, Roorkee, is an authentic record of my own work carried out during the period from June 1999 to March. 2000 under the kind supervision of Dr. Surendra Kumar, Professor, Department of Chemical Engineering, University of Roorkee, Roorkee and Dr. S.N. Sinha, Asstt. Professor, Department of Chemical Engineering, University of Roorkee, Roorkee.
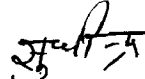
The matter embodied in this dissertation has not been submitted by me for the award of any other degree.

Dated: March 23, 2000
Roorkee

CHITRA

This is certified that the above statement made by the candidate is correct to the best of my knowledge.

S.N. Sinha
Asstt. Professor
Dept. of Chemical Engg.
University of Roorkee
Roorkee- 247667

Surendra Kumar
Professor
Dept. of Chemical Engg.
University of Roorkee
Roorkee - 247667

(i)

ABSTRACT

Reverse Osmosis (RO) is the pressure - induced reversal of the natural osmotic-flow phenomenon. While osmosis has been known for over 200 years, reverse osmosis has only recently gained commercial significance. Today its applications are numerous including purification of waste water that contain metals and salts, production of potable water from seawater, purification of chemicals, abatement of water pollution, etc.

In this dissertation, Numerical Simulation of RO process, implemented on an experimental unit, has been carried out. The unit consists of a spiral wound RO module, a UF module and a flat plate test cell. To establish the membrane performance characteristics experiments have been conducted by using salt water. The experimental observations so obtained are analyzed, and used to estimate the characteristic constants of membrane. The results of numerical simulation compare well with the experimental data.

Few Cellulose Acetate membranes were also prepared in the departmental laboratory and the structural analysis of membranes were done using S.E.M. technique.

ACKNOWLEDGEMENTS

March 2000

CHITRA

(iv)

CONTENTS

LIST OF FIGURES

NOMENCLATURE

a_1-a_5 - constants in model equations

A_w - solvent permeability constant, h/m

B_s - solute permeability constant, m/h

C - concentration, kg/m^3

J_s - solute flux, kg/m^2h

J_w - solvent flux, kg/m^2h

n - moles

ΔP - membrane pressure gradient, kg/mh^2

Q - volumetric flow rates, m^3/h

R - solute rejection

R_g - universal gas constant, $kg\ m^2/h^2k$

S_a - membrane surface area, m^2

t - time, h

T - temperature (absolute), k

u,V - volume, m^3

X - overall system recovery

Y - single-pass system recovery

π - osmotic pressure, kg/mh^2

ϕ - osmotic pressure coefficient, m^2/h^2

ψ - osmotic pressure to solute concentration ratio, m^2/h^2

Subscripts

f	-	feed
f_t	-	feed tank
f_0	-	feed at time = 0
p	-	permeate
pav	-	product, average permeate
r	-	retentate, concentrate
w	-	water
wp	-	water in permeate

INTRODUCTION

1.1 GENERAL

Membrane separation processes are increasingly being used now, where a membrane is a barrier which separates two fluids. It permits transfer of some components and not of others through it. Mechanism of transfer through membranes is by diffusion, a process of mass transfer which occurs as a movement of individual molecules. This movement may be accelerated by an electrical field, concentration, thermal or pressure gradient or by other means.

Technological advances made over the last thirty years enable engineers to perform the various membrane separation processes like Reverse Osmosis, Electrodialysis, and Ultra-filtration. These involve no phase changes, and energy consumption is very low (16).

Reverse osmosis is somewhat similar to filtration, both remove a liquid from a mixture by passing it through a device which retains the other component. However, there are at least three important differences. First, the osmotic pressure which is very small in ordinary filtration plays an extremely important role in reverse osmosis. Second there is no filter cake formation in reverse osmosis. Third, filter separates mixture primarily on the basis of size, whereas the semipermeability of reverse osmosis membrane depends on other factors such as temperature, concentration, pressure etc. (42).

In the late 1950's Reid and Breton at the University of Florida found that membranes made from cellulose acetate has the ability to reject salt. However, the water flow through these dense membrane was so low that their use in the RO process was impractical.

In the early 1960's, Loeb and Sourirajan at UCLA discovered how to make a cellulose acetate membrane with an asymetric density. This discovery permitted reverse osmosis to become the practical process today, and all commercial membranes now have the asymmetric structure in one from or another.

In 1970 Dupont commercialized RO devices containing membrane made from an aromatic polyamides (aramid) polymers, operated at a ph range of 4-11. These membrane are not susceptable to biological attack and resist hydrolysis.

In 1977 a polyamide membrane was introduced to the market in a thin film composite form. These membranes are formed by an in situ interfacial polyamide technique. The thin film composite membranes are not susceptable to biological attack and are resistant to hydrolysis, but they are much more sensitive to chlorine degradation than the aramid membranes.

Reverse osmosis handles dissolved solid concentration from a few milligram per litre to as much as 35,000 mg/l in the case of seawater desalting. But, water temperature is important because it affects the flux rate and life of membrane. Warmer water is less viscous and thus flows through the membrane faster. If feedwater temperature is expected to vary widely, then either temperature or pressure control is needed to maintain a constant flow through the membrane.

Capital cost for RO system vary widely, depending on the pretreatment, purity requirement, capacity and site-specific factors. The major energy cost is pumping power, depending on pressure level and pump efficiency. The total operating cost would also include, pretreatment processing and chemicals, RO replacement, maintenance and operating labor (29).

The commercial applications for reverse osmosis include the following:

Metal industry - Recovery of precious metals such as gold, platinum, nickel etc. from plating waste.

Textile industry - Removal of dyes, recovery of polyvinyl alcohol etc.

Paper and Pulp - Colour removal, clean water from black liquor etc.

Others - Desalting, boiler feed water treatment etc. (11).

1.2 PROCESS DESCRIPTION

Reverse Osmosis: Osmosis is defined as the spontaneous transport of a solvent from a dilute solution to a concentrated solution across an ideal semipermeable membrane which impedes passage of solute but allow solvent flow. Solvent flow can be reduced by exerting pressure on the solution side of the membrane as shown in Fig.1.1.

At a certain pressure, the osmotic pressure, equilibrium is reached and the amount of solvent which passes in each direction is equal. The osmotic pressure is a property of the solution only, provided the membrane is truly semipermeable.

If the pressure is increased above the osmotic pressure on the solution side of the membrane, the flow reverses. Pure solvent will then pass from the solution into the solvent. This phenomenon is the basis of revese osmosis treatment of water and wastewater. Useful energy per unit volume supplied to this process is in the form of pressure in excess of the equilibrium osmotic pressure (11).

In operation RO membranes are arranged so that a high pressure feed stream containing the desolved solute to be removed contacts the rejecting face of membrane so that the fluid velocity sweeps away much of retained solute from the upstream face as shown in Fig.1.2 (8).

1.3 OBJECTIVES

A Reverse Osmosis Experimental Unit has been procure from M/s Permionics, Baroda by the Chemical Engineering Department, the unit consists an UF module and a flat plate test cell. Spiral wound polyamide membrane is employed in the RO plant.

3

In order to study the RO process using the experimental unit, following objectives are formulated:

* To conduct the experiments using salt water solution

* To estimate the characteristic constants of membrane

* To conduct the numerical simulation of RO process carried out in the unit using an appropriate model

* To prepare few cellulose acetate membranes in the laboratory and study their characteristics using SEM technique.

1.4 ORGANISATION OF THE THESIS

The thesis has been organised into six chapters. Chapter II describes the history of development of membrane technology in brief, various types of RO device types of membrane and the literature review related to transport models used in predicting the membrane performance. Chapter III discuss the details of experimental set up, and the procedure for experiments on RO module and membrane preparations. Chapter IV describ the mathematical model used and procedure for estimation of parameters. Estimated parameters, Numerical Simulation of experiments are presented in Chapter V. Membrane preparation and analysis of prepared membrane are discussed in Chapter V. Finally Chapter VI highlights the main conclusions of the thesis and provides the recommendation for future work.

A-OSMOTIC FLOW   B-OSMOTIC EQUILIBRIUM   C-REVERSE OSMOSIS
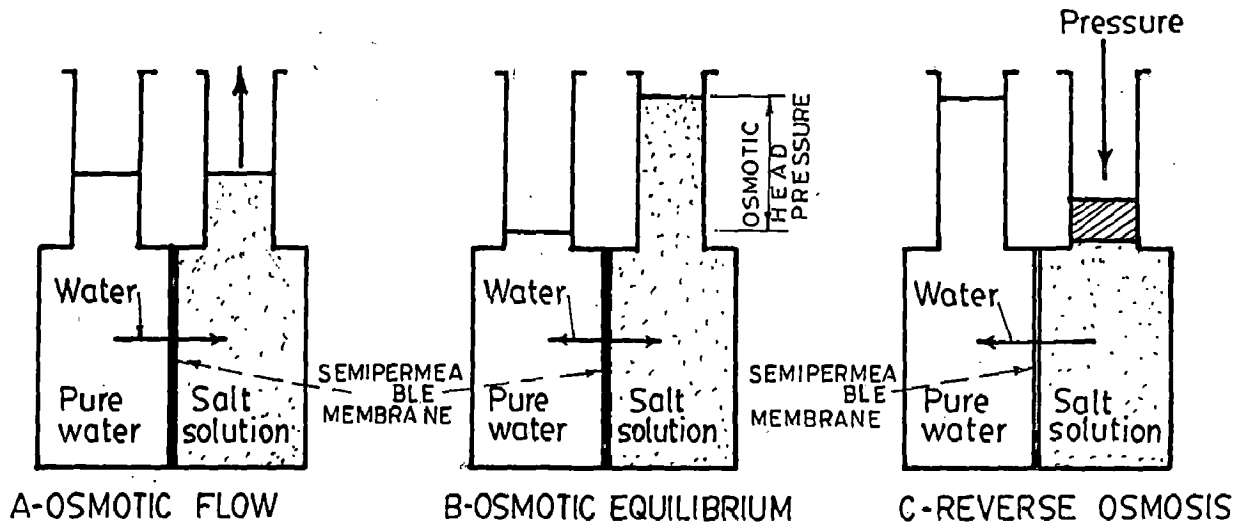
Fig. 1.1 Reverse Osmosis Process
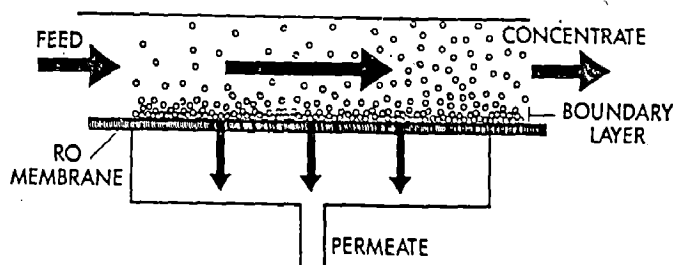
Fig 1.2 Fluid streams in RO operation.

LITERATURE REVIEW

2.1 GENERAL

Osmosis was first reported by Abbe Nollet in 1748 and was further investigated by Dutrotelot in 1827, and Vicrordt in 1848. All these researchers employed animal membranes, which were not truly semipermeable.

Pfeffer in 1877 made the first quantitative osmotic experiment using membrane of cupric ferrocynide precipitated in the pores of porcelin. This membrane was the basis for a large number of accurate osmotic pressure experiments in the late nineteenth and early twentieth centuries. Findaly in 1913 has prepared a good review of the early work on osmosis.

Theoritical development began with Vant Hoff's treatment of Preffer's results and continued under the thermodynamics work of Gibb. These developments were essentially completed by the early 1920's and it was not untill the early 1950 that interest picked up again.

Reid and Breton in 1959 conducted reverse osmosis experiments which showed that several film forming materials exhibit semipermeability to salts in brackish water and sea water. However, cellulose acetate appeared to be uniquely qualified on the basis of the rate of water produced. Later Loeb, 1962 developed a film casting technique for a modified cellulose acetate membrane to greatly increase the water flux while maintaining excellent rejection of salt. This was a major technological breakthrough which paved the way for the development of practical reverse osmosis desalination. Today, a majority of operating reverse osmosis systems contain memberanes that have been produced by the Loeb process.

In 1966 Merten et al. have presented a thorough description of the principles and practices of reverse osmosis desalination (42).

2.2 REVERSE OSMOSIS DEVICES

Three types of RO devices, namely tubular, spiral wound, and hollow fiber, are reported in literature for incorporating membranes.

2.2.1 Tubular Device

The first RO device, commercialized in the mid 1960's was tubular device using a cellulose acetate membrane. The membrane is either inserted into, or coated onto the surface of a porous tube designed to withstand the operating pressure. Feed water under pressure is introduced into the end of the tube, and the product water permeates through the membrane and the tube and is collected on the outside. The concentrated brine or reject stream exits from the far end of the tube as shown in Fig.2.1.

This device enjoyed commercial success during the late 1960s and a number of systems were installed, especially in chemical separation, food and dry processing units. However the cost of such systems because of the small membrane area per unit volume container, made them prohibitively expensive for treating large volume of solution. The tubular devices are still avaiable today and their primary use is for low-volume and high-value-in-use applications.

2.2.2 Spiral-wound Device

Typical spiral-wound RO device uses membrane in the form of a flat film. Two sheets of the flat membrane are adhered at their edges via their fabric support backing with a tricot permeate channel-cloth separating them to form a leaf as shown in Fig. 2.2. The lones are wound spirally about a plastic tube that receives the permeate from the tricot and conducts it out of the devices. Conventional spiral

cartridge or elements are 4 in. and 8 in. dia and 40 in long. Development of the spiral wound device was a major advancement in obtaining large surface area per unit volume of container.

The feed/Brine flow in a spiral device is in a straight axial path from the feed end of the cartridge to the brine end, and is parallel to the membrane surface. This feed/Brine flow pattern tends to promote concentration polarization, therefore a plastic netting is placed in the feed channel to induce some turbulence and reduce concentration polarization. Manufacturer will generally specify the minimum recommended brine flow rate for each type of device.

To achieve reasonable conversion with a spiral wound system, a number of spiral cartridge are connected in series through their product tube in pressure vessel upto 22 ft long. The vessel containing upto six cartridge arranged in this manner. The brine stream from the first cartridge in the vessel becomes the fuel to the element following it. A single stage of six cartridges in series in a vessel can be operated at conversion of upto 50% under normal circumtances. Spiral wound devices use either cellulose acetate membrane or thin film composite membrane. A spiral wound device has recently been introduced which uses an aramid membrane. Spiral devices for wastewater, brackish water and seawater are also available. The sectional view of spiral wound module is shown in Fig.2.3.

2.2.3 Hollow Fiber Device

In 1970's Du pont developed the aramid membrane and extruded it into the form of a hollow-fiber. The fiber has an asymmetric structure, with an inside diameter of about 42 μm and an outside diameter of about 85 μm. Upto 4.5 million of these fibers are gathered into a bundle as shown in Fig.2.4. During forming, epoxy adhesive is applied to one end of the bundle which after curing becomes a tubesheet. The other end of the fiber bundle is sealed in epoxy to form a tube which prevent

short-circuting of the feed stream to the brine outlet. The bundles are placed in pressure vessel upto 1.2 m (4 ft) long with diameter between 10.2 cm (4 in) and 25.4 cm (10 in).

Pressurized feed water enters the device through a porous distributor that extends length wise through the centre of the unit. The feed water passes through the distribution wall and flows radially through the fiber bundle towards the outer shell of the permeation. Water passes through the fiber wall into the fiber bore. The desalted product water flows through the bore of each fiber to the tubesheet, when it leaves the permeator. The salts and other impurities remain in the brine, which flows to the outer perimeter of the fiber bundle and exit through the brine port.

As the water flow per unit area of membrane is low, concentration polarization is not great, and hollow-fiber devices operate in the laminar flow region. Hollow fiber devices must be operated above minimum reject flow, to minimize concentration polarization and maintain an even flow through the fiber bundle. Typically a single hollow fiber permeation can be operated upto 50% conversion while meeting the minimum reject flow requirement.

The development of the hollow fiber devices was a major advancement in RO, because it permitted very large membrane area per unit volume. Thus reverse osmosis sytem that employ the hollow fiber device are the most compact (29).

2.3 TYPES OF MEMBRANE

Membrane is a phase, which acts as a barrier to flow of molecular or ionic species between other phases that are usually heterogeneous, either a dry solid, solvent, swoolen gel or a liquid that is immobilized. It must transport some molecules faster than others, must have high permeability for some and low for others, must employ highly perm selective membrane transport mechanism (42).

Membranes may be categorised in various ways as discussed below:

(a) **Artificial:** All membrane involved in membrane operation are supposed to be artificial. The term artificial is more general than the term synthetic and includes some natural materials having structure like those of a membrane, modified by man through biological, chemical or physical treatments.

(b) **Anisotropic:** Membrane where the separation takes place in one or more thin taut skins (active layers), supported by substructure with pores much larger than those of the active skin.

Usually membrane used for reverse osmosis, ultrafiltration and to some extent microfiltration contains a dense skin on one side, so that they can also be characterized as asymetric membrane. The term anisotropic is more general covering the case of some gas separation membrane which have skins on both sides.

These can be symmetric but not isotropic Anisotropic hollow fibres, especially show radial anisotropy, while membranes in other configuration show transversal anisotropy.

The opposite to anisotropic membrane are isotropic membranes, where the porosity is the same in all directions. Anisotropy does not necessarily imply a variation of a property in all directions, and in fact with membrane the anisotropy is one-dimensional.

(c) **Composite membranes:** Membrane made from composite materials meant for any inhomogeneous mixture of polymer or polymers and other materials. Composite membranes can be prepared not only by the deposition of a polymer film but also by the reaction or adhesion of a solution on a substructure.

10

The term composite materials is any possible combination of materials, e.g. ceramic membrane with a metal oxide overlay.

(d) Dynamic membrane: Membrane in which an active layer is formed on the membrane suface by the deposition of substance contained in the fluid to be treated. Substance which are usually used are inorganic oxides such as Z_rO_2 and added polymers. The term dynamic membrane is in use in the USA and Japan.

(e) Permselective membrane: Membrane which separates component of a fluid by means of differences in one or more properties of the component such as size and shape, electrical charge, solubility and diffusion rate. Historically, the term semipermeable membrane has been used without having a well defined scientific meaning. Later this term has been mainly related to the simple mechanism of separation according to size and shape while the term permselective has been applied to electrodialysis membrane which are selective according to electrical change (41).

(f) Synthetic membrane: Membrane made of man made polymers exhibiting a coarse, porous, fine porous or dense structure, may exist with one of the following four organization: homogeneous, asymmetric, asymmetric provided with a skin at the top surface or composite, as shown in Fig.2.5. To some extent, a homogeneous organization is a limiting case. In general coarse and fine porous membranes possess an asymmetric organization exhibiting a porosity (43) gradient across the membrane which may, however, be more or less pronounced. In case of a very weak porosity gradient, it is nearly impossible to differentiate such membranes from completely homogeneous ones. In case of fine porous membrane, two kinds of asymmetric organization might exist. In the first the membrane exhibit only a porosity gradient, whereas in the second case, the membrane passes a dense layer (active layer) on top of an asymmetric fine porous matrix. Commercially available

11

RO membranes exhibit an asymmetric or a composite organization where a porous matrix (support) is tapped by a more or less dense layer (active layer, thin film). The transport properties of asymmetric and composite membranes are essentially controlled by their active layer.

2.4 CELLULOSIC AND NON CELLULOSIC MEMBRANES

Since membrane first made their appearance in chemical and microbiological laboratories as an efficient tool for the separation of molecular mixtures more than 40 years ago, considerable effort has been spent by engineers, physicists and chemists to develop better membranes and to extend their range of application. In the early days of membrane separation processes, only microporous structures were used commercially in microfiltration and dialysis. A short time later cation and anion exchange membranes were developed and successfully employed in electrodialysis for the desalination of aqueous solution and finally, with the discovery of asymmetric membrane and its use in ultra and hyper filteration, membranes have changed from a scientific and laboratory curiosity to an industrial tool with significant technical and commercial impact.

The usefulness of a membrane in a mass separation process is determined by its selectivity, chemical, mechanical and thermal stability, and overall mass transport rate (22).

The ideal membrane for desalination by RO would consist of an ultrathin imperfection free film of a polymeric material. The transport properties of the material would be such that water could pass through with little hindrance, while presenting a virtually impermeable berrier to salt. Most polymers approximate this ideal behaviour by exhibiting different flow rates, or different permeabilities to water and salts. In order for water and simple salt to be transported across the barrier they must first dissolve and penetrate into the polymer material.

12

To provide a larger flow rate of water, a real membrane must be extremely thin, ideally not more than a few Angstroms thick. Conversely, the membrane must be extremely strong in order to withstand the driving pressure of the in comming feed stream. These requirements are incompatible and led to the development of various support methods. These substrate included woven and unwoven fabric, resin starved fiberglass, porous ceramic, hemp paper and microporous plastic, such as polysulfone. Commercial polymer candidates have been CA, CTA blends of diacetate and triacetate, polyamide (PA) and more recently composite membranes of polyamide and polyurea (32).

2.5 TRANSPORT MODELS

The general purpose of a membrane mass transfer model is to relate the performance (usually expressed in terms of flux of solvent and solute) to the operating conditions (usually expressed in terms of pressure and concentration driving forces). In the model some co-efficients emerge that must be determined based on the experimental data. The success of a model can be measured in terms of the availability of the models to describe mathematically the data with co-efficients that are reasonably constant over the range of operating conditions.

A. Phenomenological Transport Models (PTM)

Models which are independent of the mechanism of the transport are known as PTM. These models are based on the theory of irreversible of thermodynamics.

(i) Irreversible Thermodynamics - Phenonenological Transport Relationship

In the absence of any knowledge of the mechanism of transport or the nature of the membrane structure, it is possible to apply the theory of irreversible thermodynamics to membrane systems. In IT, the membrane is treated as a black box. Models stating the relationship between forces acting on the system and the flux of material through the membrane are formulated. For system that are not far from

equilibrium, IT suggests reasonable choices for forces and fluxes. The phenomenological rationships are manageable ways of expressing the relationships between the observed fluxes and the applied forces.

(ii) Irreversible Thermodynamics - Keden Spiegler Relationship

One critical assumption in the relationship between IT and phenonenological transport is that the linear laws were assumed to apply over the whole thickness of the membrane. Spiegler and Kenden resolved the problem of rewritting the original linear IT equations in differential form and then integrating them over the thickness of the membrane.

B. Nonporous Transport Models (NTM)

Models in which it is specifically assumed that the membrane is nonporous.

(i) Solution-Diffusion Relationship

The SD model was originally applied to reverse osmosis by Merten and co-workers. The membrane surface layer is considered to be homogeneous and nonporous. Transport of both solvent and solute occurs by the molecules dissolving in the membrane phase and then diffusing through the membrane. The permeability of a species is equal to the product of the solubility and the diffusivity for that species.

(ii) Solution-Diffusion Imperfection Relations

The solution diffusion imperfection model (SDI) was driven by sherwood et. al. The premise of this model is that during the membrane making process small defects in the membrane surface structure could result and these defects would lead to leakage of solution through the membrane. This mechanism would account for membranes that exhibited lower separation than the separation calculated based on solubility and diffusivity measurements.

14

(iii) Extended Solute-Diffusion Relationship

Burghoff et al. and Jonsson pointed out that in the original SD model, a pressure term in the solute chemical potential equation was neglected. The complete expression for chemical potential, including the pressure term, is:

$$\Delta \mu_A = RT \ln \left(\frac{C_{A2}}{C_{A3}} \right) + V_A \Delta P$$

Where $\Delta \mu_A$ is the solute chemical potential differences across the membrane and V_A is the solute partial molar volume. In general, to neglect the pressure term, $\ln(C_{A2}/C_{A3})$ must be significantly greater than $V_A \Delta P/RT$.

C. Porous Transport Models (PTM)

Models in which it is specifically assumed that the membrane is porous

(i) Kimura Sourirajan Analysis

The Kimura-Sourirajan analysis (KSA) was developed based on the preferential sorption-capillary flow mechanism proposed earlier by Sourirajan. According to the KSA relationship, the membrane surface is microporous and transport occurs only through the pores. The membrane has a preferential attraction for water, and the resulting sorbed layer of almost pure water is forced through the membrane pores by pressure. Therefore, solute separation and flux are determined both by physicochemical interaction between the solute solvent membrane system and by the number, size and size distribution of pores.

(ii) Finely - Porous Model

The finely-porous model developed by Merten, is based on a balance of applied and frictional forces, as first proposed by Spiegler, in a one-dimensional pore. A complete derivation of the model has been given by Jonson and Boesen and by Soltanieh and Gill.

(iii) Two Dimensional Pore Flow Models

Several authors have considered transport of solute and solvent in two-dimensional right cylindrical pores. The advantage of using a model of this type is that the model should more accurately describe the transport in a porous membrane. The disadvantage are that the modes are considerably more complex (usually involving advanced numerical techniques to solve the governing equations) and the model are still considerable simplification of the real situation (8).

Calculation of actual fluxes in reverse osmosis desalination through membrane tubes involves considerable iteration due to the existance of concentration polarization. Goruganthu H. Rao and Kamalesh K. Sirkar developed explicit flux expressions on the basis of the flux expression of Lonsdale et al., Sourirajan, and Johnson et al. to eliminate iteration. Low levels of solvent flux in existing membranes allow approximations leading to such explicit expressions. The computer flow diagram for reverse osmosis plant design with membrane tubes in series has been simplified by means of the explicit flux expressions (17).

The effect of operating parameters (transmembrane pressure, flow rate, temperature and feed concentration) on the performance of a spiral-wound and a tubular thin-film composite reverse osmosis (RO) membrane during the concentration of milk was studied by M. Cheryan et. al. No permeation was obtained until the applied transmembrane pressure exceeded the osmotic pressure of the feed. With all modules, flux increased linearly with applied transmembrane pressure upto about 2.1 to 2.8 MPa. Flux then because asymptotic and decreased at much high pressures. The pressure at which maximum flux was obtained, was higher with higher flow rate (30).

In comparison to cellulose acetate, the composite membrane gave higher flux and better rejection of salt and sugars; the difference in permeate quality was greater at higher concentration factors. Flux declined with feed concentration, as

16

expected for an osmotic pressure limited system. Under otherwise equavilent operating conditions, higher flux could be obtained with the tubular unit but at the expense of higher energy consumption. Substantial energy savings are possible by incorporating RO in certain milk evaporate and dehydration plants, depending on the design of the evaporation system (30).

A method for calculation of ultrafiltraion and reverse osmosis processes has been developed by Harri Niemi and Seppo Palosarri to enable the calculation of permeate flux and rejection at different pressures and concentrations. The method has been combined with a process simulation program which calculates all streams of the process. Permeate flux and rejection in membrane processes are dependent on pressure and concentration of the solution. This dependence has to be known in the simulation of these processes. Normally a considerably large number of time consuming experiments have to be made to find the dependence of permeate flux and rejection on pressure and concentration. In this work the minimum experimental information was determined to enable the calculation of permeate flux and rejection. Two calculation procedures, one based on the finely porous model and the other on the statistical mechanical model, were used. In these models permeate flux and rejection are described by four quantities. The values of these quantities are constant for each separation system having the same solution, membrane and temperature. A method of obtaining the values of these quantities from experiments is described and the minimum experimental information was determined to enable the calculation of permeate flux and rejection over the entire operating range of the process (19).

Harri Niemi and Seppo Palosaari, developed a membrane separation model for tubular module reverse osmosis and ultrafiltration processes. The membrane area of a process can be calculated by this model and the stream matrix of a process can be

17

determined by a process simulation program. In this work the UNICORN simulation program was used. The membrane separate model calculates permeate flux and rejection of the solute in small increments of the membrane tube over the entire range of the tube and the process. Calculation of the permeate flux and rejection can be performed by polynomial equations fitted to the experimental data, or by equations based on mass transfer moddels. The finely porous model and the statistical mechanical model was used. Some experimental data are also needed for determining the parameters of the mass transfer model equations by parameter fitting (18).

Takehito Kataoka et al., proposed permeation equation based on the solution diffusion model for pervaporation, vapor permeation and reverse osmosis on the different assumption about the pressure gradient inside a membrane: a flat gradient and a linear gradient. With these equations the permeation properties in PV, RO and VP can be estimated once the transport parameter of a membrane is known.

The effect of upstream pressure on selectivity and flux in RO and PV was estimated by sample calculations for water and ethanol selective membranes in ethanol water system. Flux and selectivity in RO is smaller and, reaching that in PV at infinite pressure (38).

Fig. 2.1 Tubular device

Brine

Anti telescoping device

Product

Product tube

Brine

Fiber glass outer wrap

Feed channel spacer

Brine seal

Feed

Tricol product water collection channel

Membrane surface

Membrane support backing

Product

Product flow

Adhesive

Feed

Membrane surface

Brine seal carrier
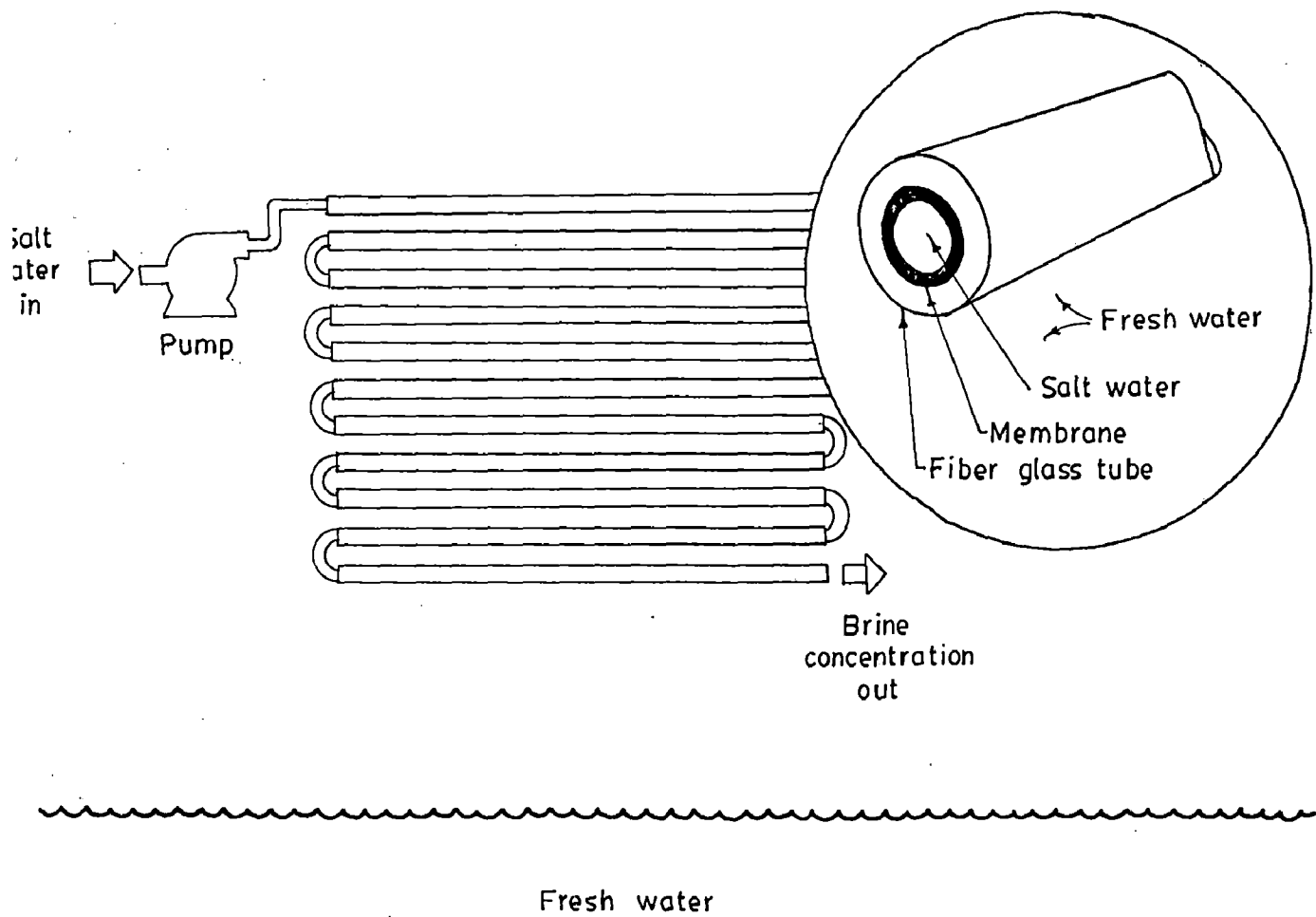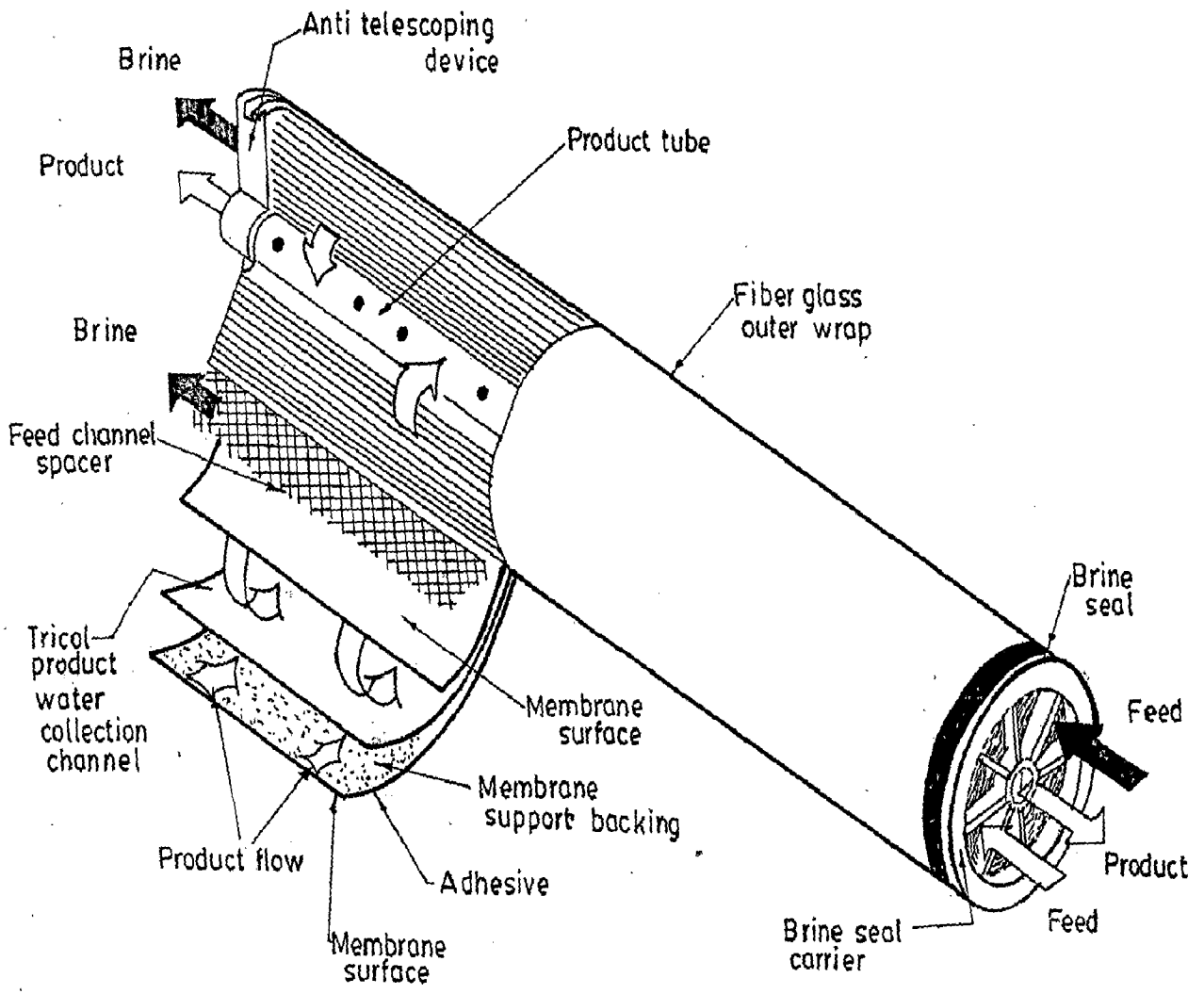
Fig. 2.2 Spiral wound device

20
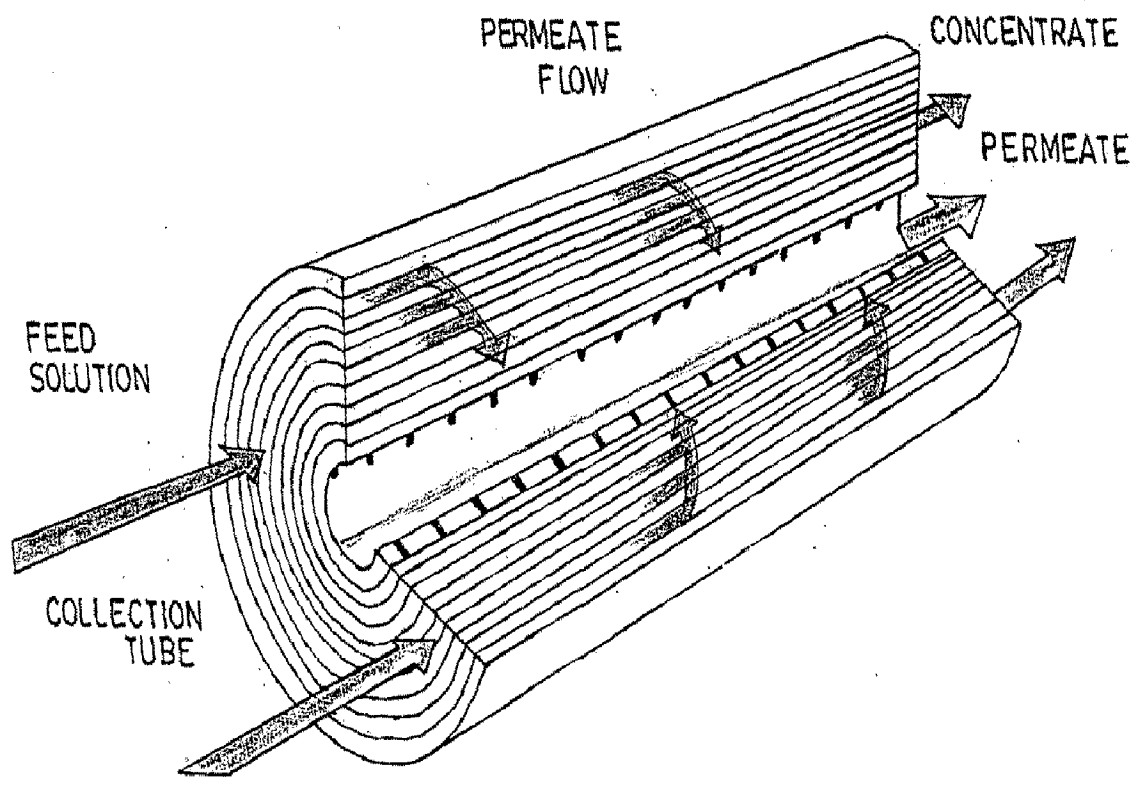
Fig. 2.3 Spiral wound membrane element section view

42 um
(0·0016 in)

85 µm
(0·0033 in)

Thin skin
0·1 - 1·0 µm thick

Porous
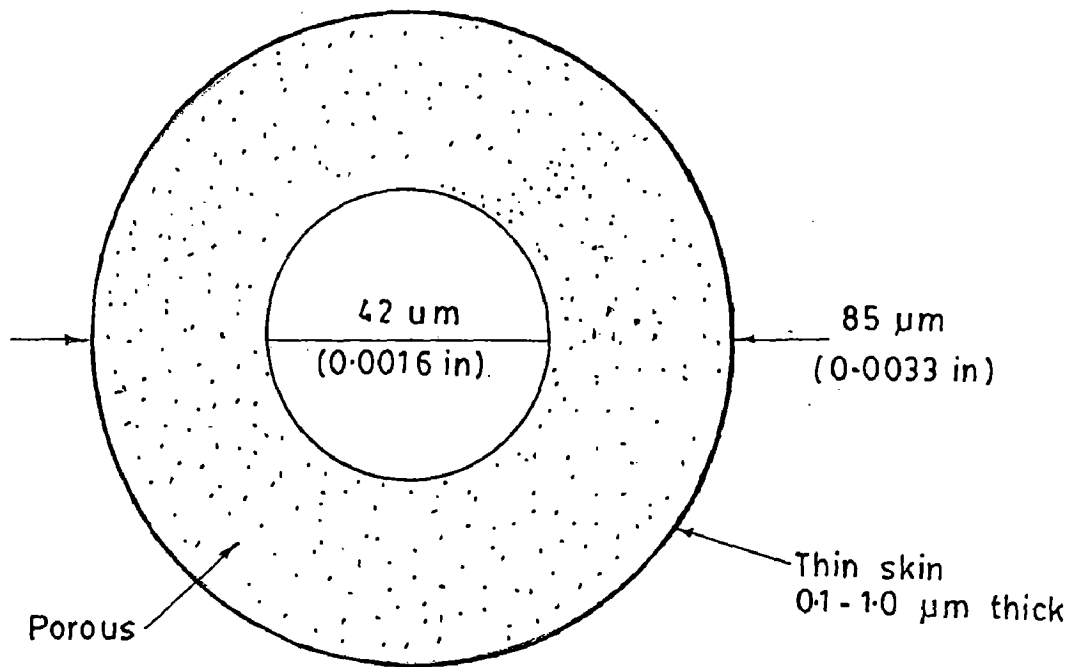
Fig. 2.4 Hollow fiber device

22

Homogenous Membranes

Asymmetric Membranes

active layer

porous
sublayer

Composite Membranes

active layer

gel layer

porous sublayer
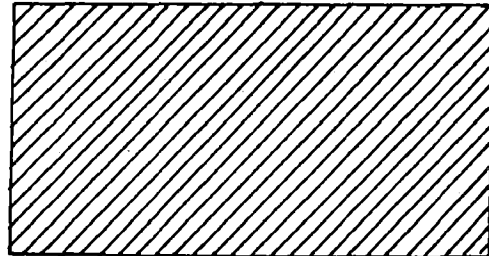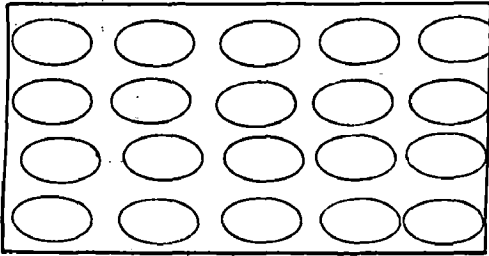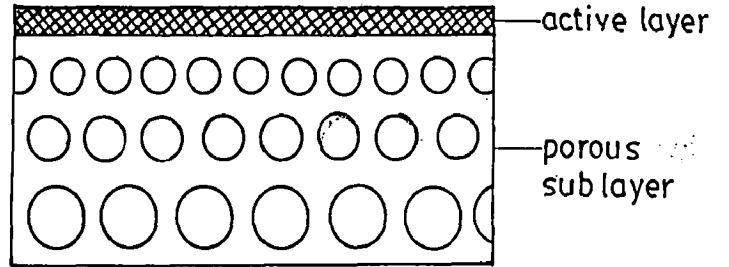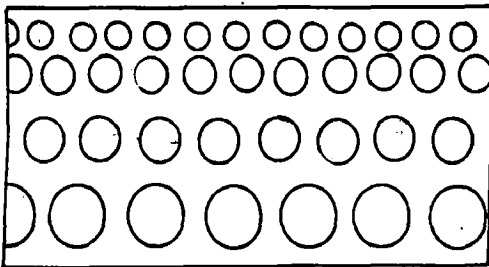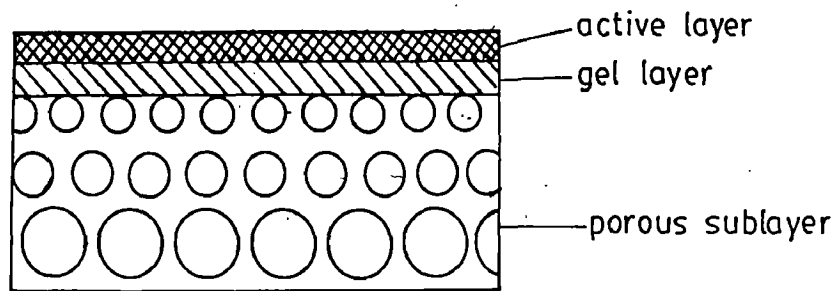
Fig. 2.5 Digrammatic presentation of basic membrane structures

and membrane organisation

23

EXPERIMENTAL UNIT AND PROCEDURE

3.1 EXPERIMENTAL UNIT

The experimental unit has two modules one for Reverse osmosis and other for ultrafiltration process. One test cell is also provided to test different membranes.

3.1.1 Description

The schematic diagram of the experimental unit is shown in Fig.3.1. Feed, permeate, retentate tanks, RO module, pump, motor, in and out pressure gauges, valve, inlet header, outlet header, hgih pressure cut out, starter are shown in figure. During operation feed goes from feed tank to pump from where pressurised feed comes to inlet header. From inlet header it goes to RO module. Feed comes to outlet header from RO module. If permeate and retentate are collected in separate tanks it is called unsteady state mode of operation. If retentate and permeate are collected in the feed tank itself, it is called steady state mode of operation. High pressure cut out is provided for safety purpose. If pressure exceeds beyond certain limit it stops the motor automatically.

3.1.2 R.O. Unit

The Elevation, Plan and side view of the experimental unit are shown in (31) Figure 3.2, 3.3 and 3.4 respectively. The itemized list of the unit is as follows:

(1)	Angle Stand	As per drg.
(2)	Pressure Vessel	$73^{0/D} \times 63^{1/D} \times 25''$ Lg
(3)	Module	25 25 PA RO

(4)	Pressure Vessel	$73^{O/D}$ x $63^{I/D}$ x 25" Lg
(5)	Module	25 25 PS UF
(6)	Inlet Pressure Gauge	0 TO 400 psi
(7)	Outlet Pressure Gauge	0 to 400 psi
(8)	Gate Valve	1/2" NB x std
(9)	Test Cell	As per drg.
(10)	Pump	960 rpm
(11)	Pump Pulley	8" ϕ x B Type
(12)	Motor	1.5 HP, 925 rpm
(13)	Motor Pulley	3" ϕ x B - Type
(14)	V Belt	61" B - Type
(15)	BPR	3/4" NB x std
(16)	High pressrue cut out	0 to 430 psi
(17)	Damper	4" ϕ x 10" Lg
(18)	SS Braided pipe	1/2" NB x 24" Lg
(19)	High Pressure pipe	1/2" NB x 24" Lg
(20)	Quick release coupling	1/2" NB x std
(21)	Starter	Type Mk-1
(22)	Inlet header	1" NB x 14G x 640 Lg
(23)	Outlet header	1" NB x 14G x 540

3.1.3 Membrane Specification

(a) RO Unit

The RO module is made from polyamide membrane. The module is of spiral-wound type. The specification for RO module is given as follows:

(i)	Length	40.64 mm
(ii)	Width	50.8 mm
(iii)	Diameter	6.35 mm

25

(iv)	Pore size	0.001 μm
(v)	Thickness	0.002 - 0.003 mm
(vi)	Packing	Netlon - mesh

(b) Test Cell

A rectangular size, flat sheet is used in test cell. The specification (31) for this type of membrane is as follows:

(i)	Length	15.24 mm
(ii)	Width	10.16 mm
(iii)	Packing	SS - Mesh and carrier cloth

3.1.4 Cleaning Agents

Frequent cleaning is necessary for better performance of the membrane. The cleaning agents for polyamide membrane are given as follows:

(i)	Sodium Metabisulfate	1% solution in water
(ii)	Trisodium Phosphate	1% "
(iii)	Sod. Lauryl Sulphate	0.1% "

3.1.5 Operating Parameters

Feed flow rate, pressure and temperature are important operating parameters: their maximum limits are given below:

(i)	Feed Flow Rate		15 litre/min
(ii)	Operating Pressure	(a)	200 psi for RO Module
		(b)	100 psi for UF Module
		(c)	For membrane test cell, maximum pressure depends on the type of membrane used.
(iii)	Temperature		45°C

26

3.2 EXPERIMENTAL PROCEDURE

Experiments have been conducted using RO device.

A simple lab or pilot scale system can be operated in several modes. Fig.3.5 describes the flow option for the experimental system used in this analysis.

The simple process case of a once through, continuous mode of operation is run most easily. Under this type of operation, feed characteristics remains the same and the retentate concentrate, and permeate are both collected separately. In a semi-bath unsteady state mode of operation, retentate is recycled to the feed tank and permeate is collected separately (12).

3.2.1 Experiments on RO Module

Experiments have been conducted on RO module in the following situations:

* Unsteady state mode of operation.

* Steady state mode of operation for the calculation of solute permeability constant.

The data have been obtained for various solute (salt) concentration of feed (0.2% - 0.8%) under both the above situation. Feed flow rate is maintained between 12-14 litre/min., and is measured by the usual method of noting the time for the collection of a known volume of solution. These are reported in tabular form in appendies B and C respectively. Salt concentration in the solution is determined by measuring its conductivity by conductivity meter. Calibration curve is given in appendix-A, and correlation is as given below

$$y = 0.0641 \ x - 0.0094, \quad R^2 = 0.9957$$

where x = conductivity of solution, mmho

y = % salt concentration

Further, experimental data, required for the calculation of osmotic pressure of solute concentration ratio, and solvent permeability constant, have been taken. These are given in appendix-D.

3.2.2 Membrane Preparation

Cellulose Acetate membranes were prepared in the laboratory. The process involves the following steps:

Ist Step: Preparation of Casting Solution

The relative proportion of the cellulose derivative in the casting solution (32) may range from 18 to 30% by weight, while the remaining weight percentage is contributed by the solvent, such as Di-methyl Sulfoxide, Di-methylformamide, Acetic Acid, Acetaldoxime and Diacetone Alcohol or a solvent, additive mixture composed of acetone and formamide, or a mixture of acetone and glyoxal. A cellulosic solution composed of from about 18 to 30% by weight of cellulose acetate, from about 33 to 52% by weight acetone and from about 18 to 48% of formamide has yielded dry membranes which upon use in reverse osmotic systems have exhibited an excellent balance between the yield of treated water and the desalination or separation effected thereby. Membrane was cast from a solution composed of the following ingredients.

Cellulose Acetate	25%	Cellulose Acetate	60 gm
(Acetic acid content 40%)		(Acetic acid content 50%)	
Formamide	30%	Formamide	50 ml
Acetone	45%	Acetone	50 ml
		Magnesium Chloride	20 gm

The contents were mixed in a plastic bottle and were kept overnight. After 10-15 hours more acetone was added and mixed.

IInd Step: Casting of Membrane

Membrane was casted on a glass plate with the help of a glass rod on a cloth. Cello tape is fixed to the three sides of the plate for uniform thickness of the membrane. Too slow a period of time permits excessive evaporation. Too fast a sweep time results in imperfect surface formation or even rupture of the film.

IIIrd Step: Evaporation

After casting the membrane it was left for air drying. Film casting and subsequent solvent evaporation into the air is accomplished most conveniently and effectively at reduced temperature, which reduces the solvent evaporation rate and permits effective initiation of the desired organisation of the water-cellulose acetate structure. Too short time prevented the formation of a firm film.

IVth Step: Quenching

After a predetermined time such that the solvent is not completely evaporated, the film is immersed in water, preferentially but not essentially in ice water, to prevent complete air drying of the film. Complete air-drying has been found to be harmful in that it reduces the desalinizing capacity of the film and is believed to damage the water cellulose acetate structure which has been initiated.

Vth Step: Annealing

Finally the film is preferably heated prior to use to complete the oranization of the film for high flow desalinization. A preferred technique for heating the films consists in setting them or placing them under water on glass plate. The film after heating in the water bath is left there for a period of time before being taken out to use. The water bath temperature is 70°C.

29
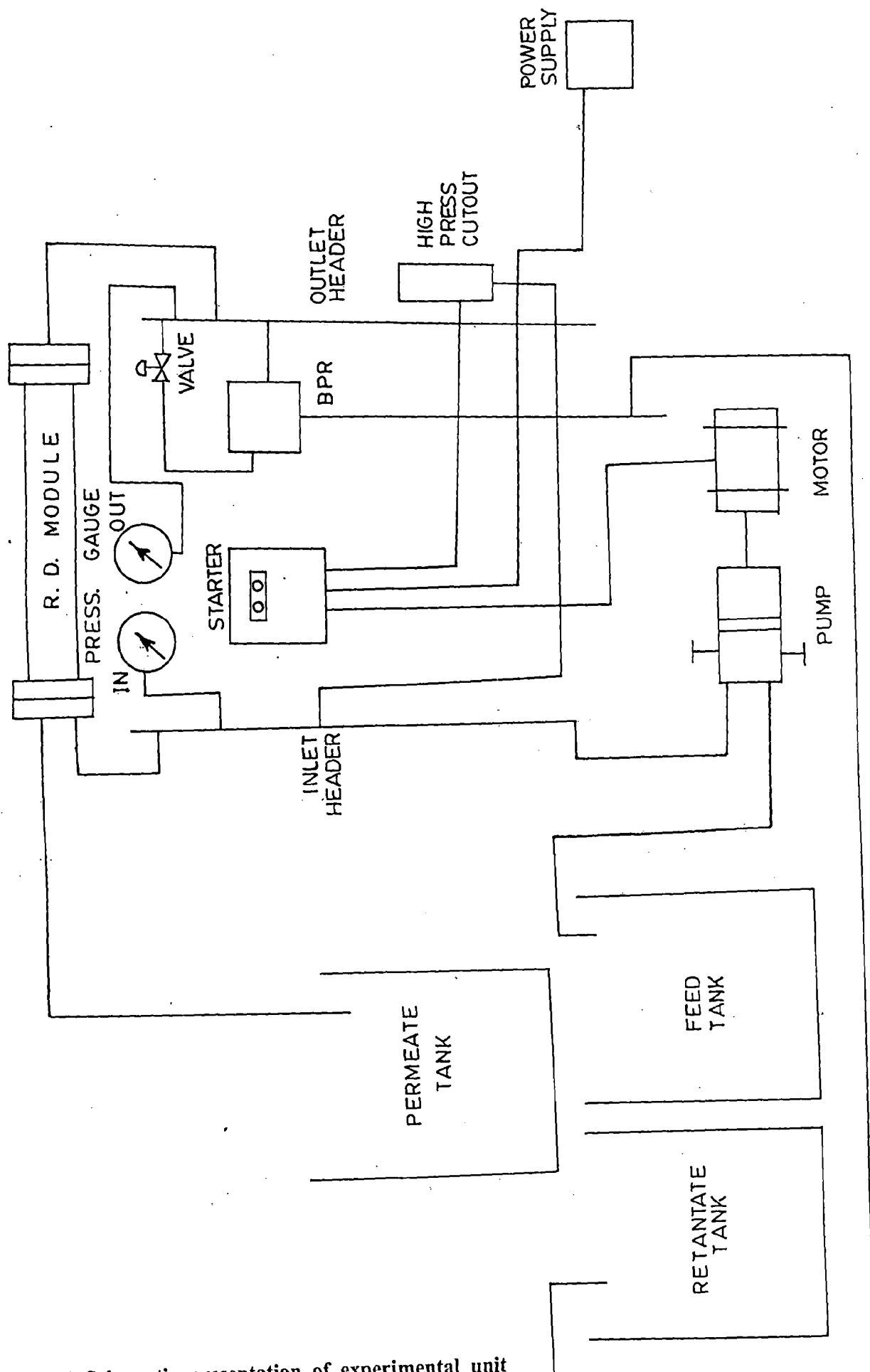
Fig. 3.1 Schematic presentation of experimental unit

30

Fig. 3.2 Elevation

31

Fig. 3.3 Plan

32

RO

UF

PLUG POINT

Fig. 3.4 Side view

33
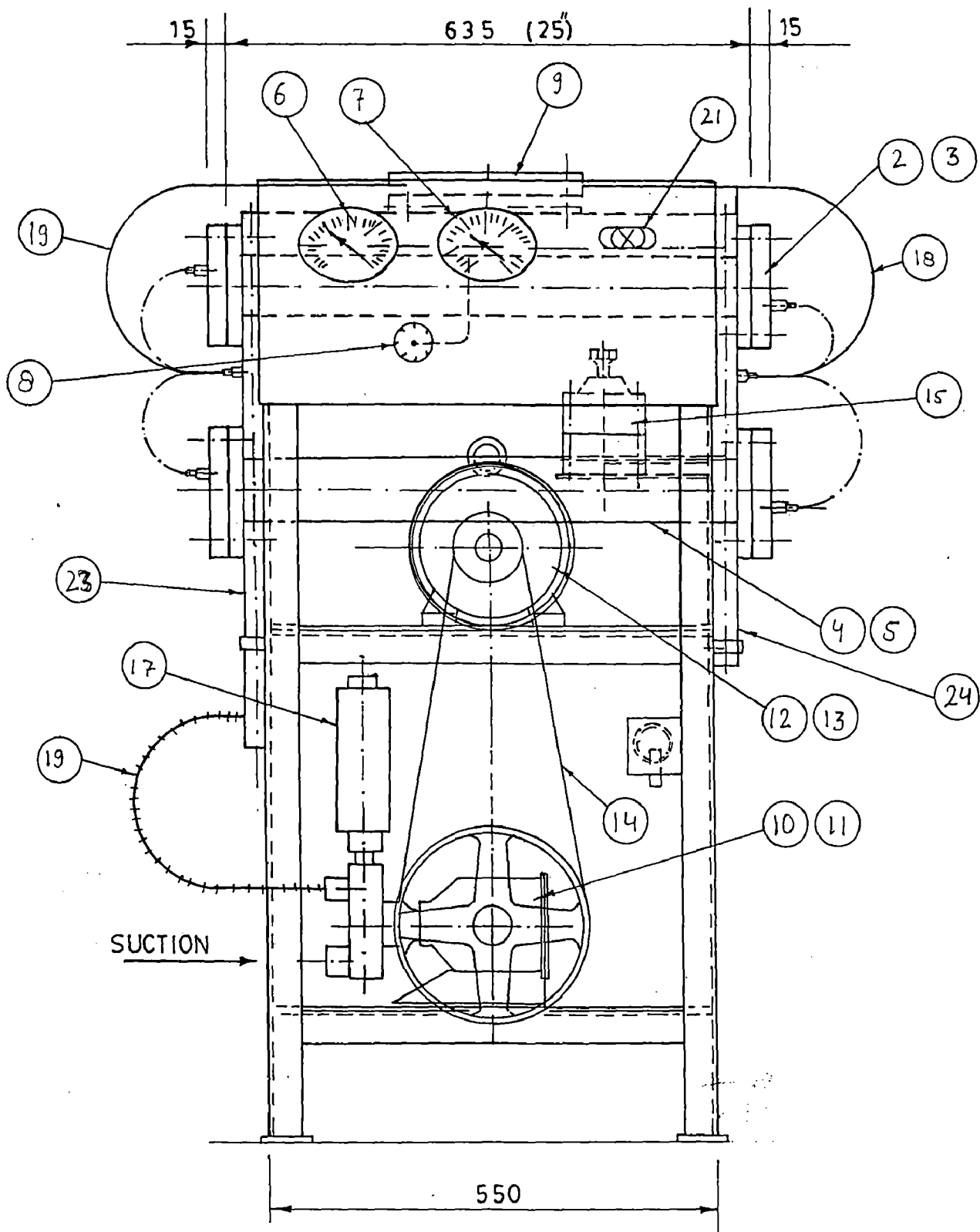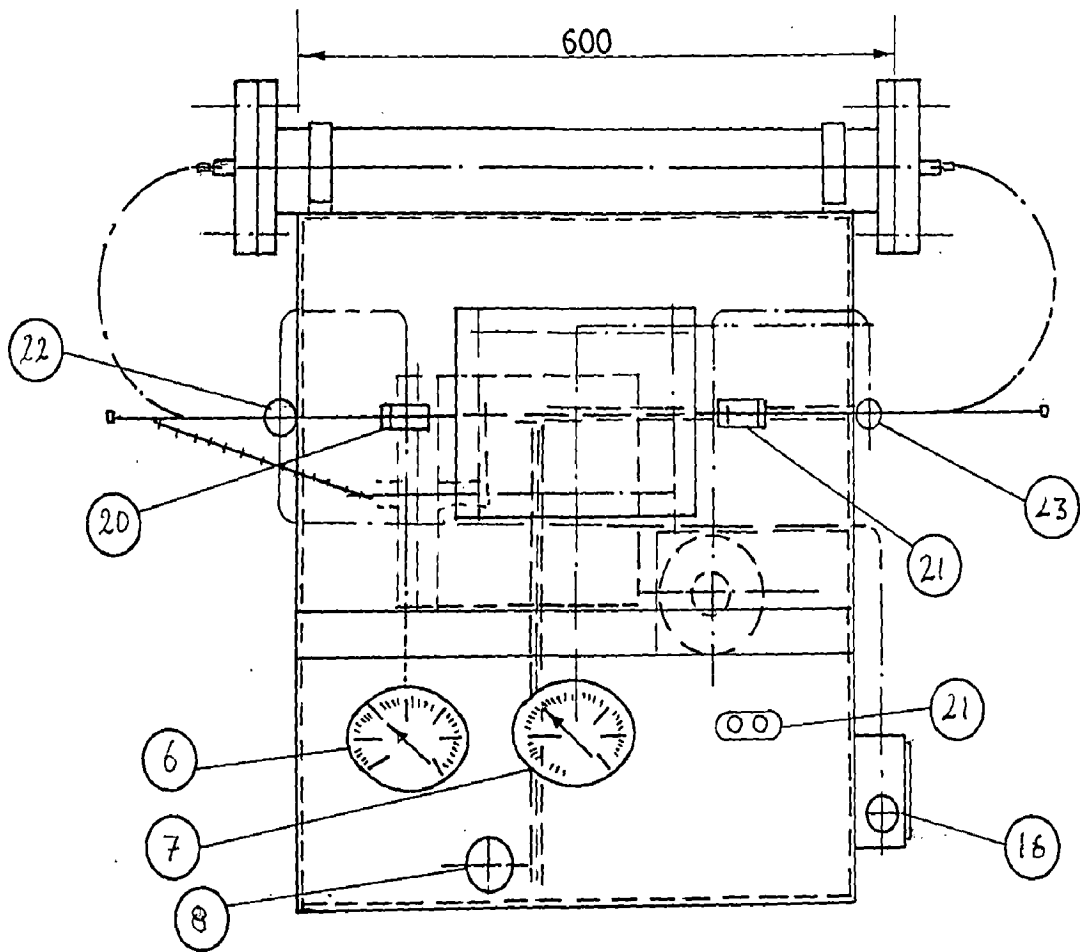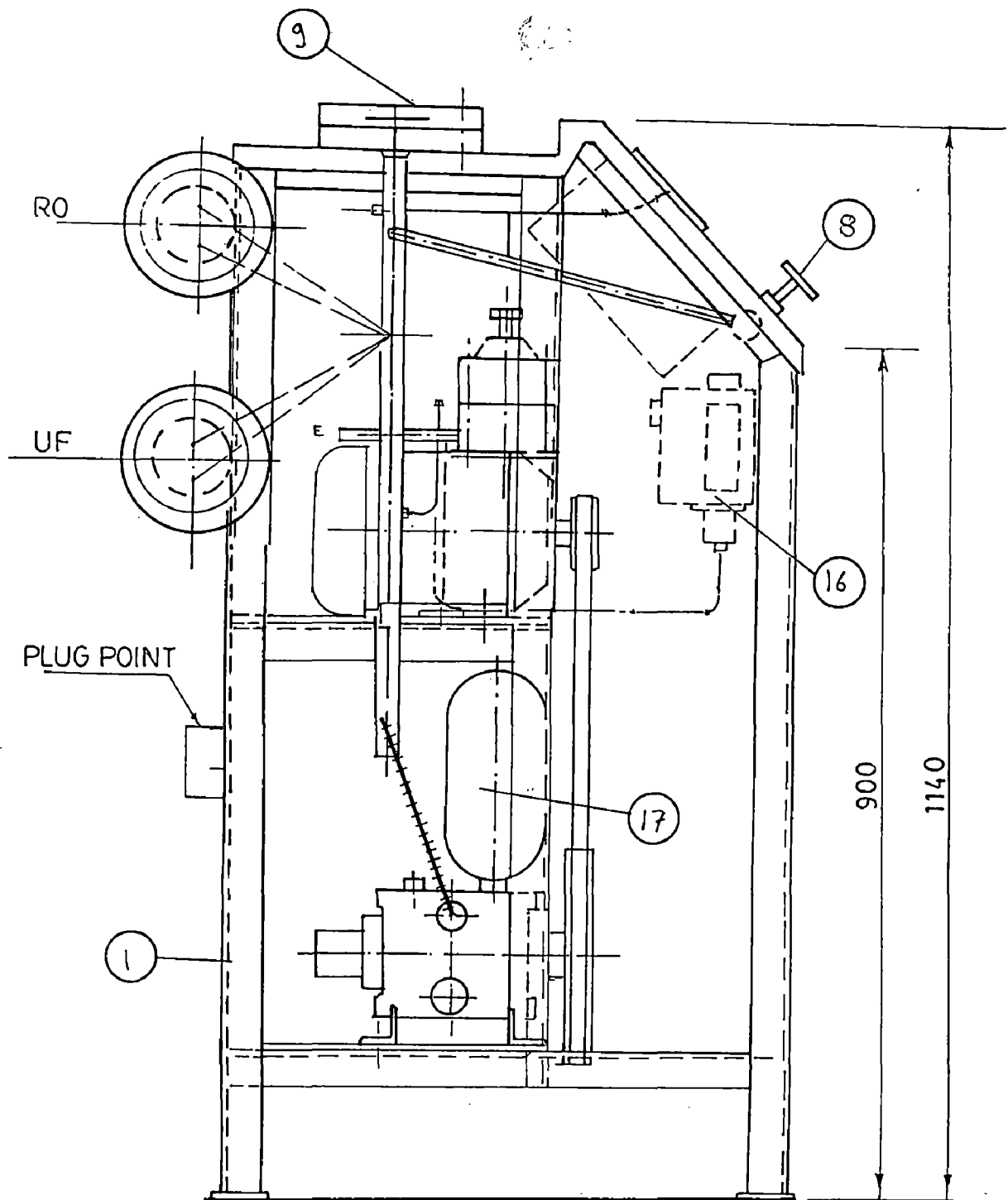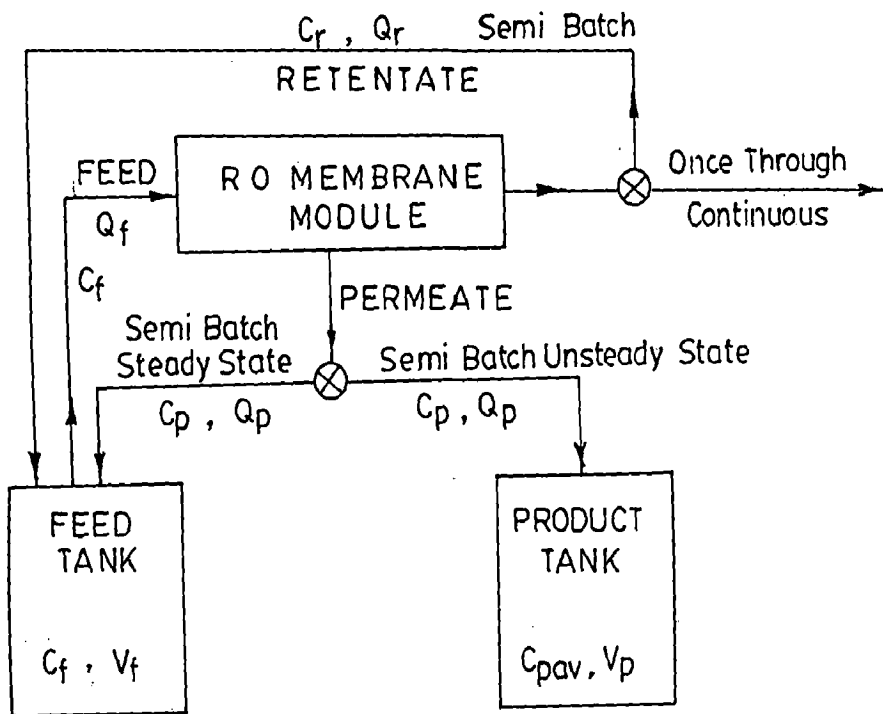
Fig. 3.5 Modes of RO system operations

MATHEMATICAL MODEL USED AND PROCEDURE FOR ESTIMATION OF PARAMETERS

This chapter describes the mathematical model used in numerical simulation for RO process, and also the procedure used for estimating model parameters.

4.1 MATHEMATICAL MODEL

C.S. Slater et al., 1985 developed a simulation model and verified for a small scale reverse osmosis system operating in closed-loop concentrating mode. The model combines material balances on the feed tank, membrane module and product tank with membrane mass transfer models. The proposed model is a nonlinear differential equation representing the feed concentration as a function of operating time. Correlation of flux, solute concentration, and rejection with operating time and overall system recovery are function of the model. Total dissolved solids (TDS) was the parameter representing solute concentration. Data from simple salt and industrial wastewater experiments were used to verify the model. The model suggests a good fit to the data over the range studied. The model equation are given from eqn. (1) to eqn. (35).

The flow of the solvent through the membrane is defined in terms of flux

$$J_w = \frac{Q_p}{S_a} C_{wp} \tag{1}$$

J_w = solvent flux, Q_p = Vol. production rate of permeate

S_a = membrane surface area, C_{wp} = concentration of water in permeate

$$J_w = A_w (\Delta P - \Delta \pi) \tag{2}$$

ΔP = hydraulic pressure applied across the membrane

$\Delta\pi$ = osmotic pressure

J_s = $B_s\Delta C$ (3)

ΔC = $C_f - C_p$ (4)

J_s = solute flux, B_s = solute permeability constant,

ΔC = difference in solute concentration across the membrane

C_f & C_p feed and permeate concentration

$$R = \frac{C_f - C_p}{C_f} = 1 - \frac{C_p}{C_f} \quad (5)$$

R = rejection

$$C_p = \frac{J_s C_{wp}}{J_w} \quad (6)$$

$$R = 1 - \frac{J_s C_{wp}}{J_w C_f} \quad (7)$$

Substitution of solute and solvent flux expression and rearrangement gives

$$R = \left[1 + \frac{B_s C_{wp}}{A_w(\Delta P - \Delta\pi)}\right]^{-1} \quad (8)$$

Material balance on product tank yields Fig.3.5.

$$Q_p C_p = \frac{d(V_p C_{pav})}{dt} \quad (9)$$

C_{pav} = avg. product concentration

$$Q_p C_p = \left(\frac{dV_p}{dt}\right) C_{pav} + \left(\frac{dC_{pav}}{dt}\right) V_p \quad (10)$$

Initial conditions for this relationship are

V_p = 0 are C_{pav} = C_p at t = 0

$$\frac{dV_p}{dt} = Q_p \quad (11)$$

Substituting in Eq. (10)

$$Q_p(C_p - C_{pav}) = \left[\frac{dC_{pav}}{dt}\right] V_p \tag{12}$$

The material balance around the membrane module becomes

$$Q_p C_p = Q_f C_f - Q_r C_r \tag{13}$$

The subscript f, p, and r refer to feed, permeate and retentate respectively.

Balance around feed tank becomes

$$Q_r C_r - Q_f C_f = \frac{d\ (V_{ft}\ C_{ft})}{dt} \tag{14}$$

V_{ft} = volume of the feed in the tank with a tank concentration of C_{ft}.

At any instant of time t, $C_{ft} = C_f$. Combination of eqn. (13) & (14)

$$-Q_p C_p = \frac{dV_{ft}}{dt} C_f + \frac{dC_f}{dt} V_{ft} \tag{15}$$

$$-\frac{dV_{ft}}{dt} = Q_p \tag{16}$$

and $V_{ft} = V_{f_0}$ at t = 0

Integrating eqn. (16)

$$V_{ft} = V_{f_0} - Q_p t \tag{17}$$

$$-Q_p C_p = Q_p C_f + (V_{f_0} - Q_p t)\frac{dC_f}{dt} \tag{18}$$

Relationship between the material balance and mass transfer models:

The model is based on the Vant's Hoff expression

$$\pi = \phi\ (n/V)\ R_g T \tag{19}$$

ϕ = osmotic pressure coefficient

(n/v) = molar concentration

R_g & T = universal gas constant and absolute system temperature respectively

Assuming constant temperature and incorporating the other constant into an osmotic pressure to solute concentration coefficient, ψ.

$$\pi = \psi C \tag{20}$$

ψ = constant over the operating range

$$J_w = A_w [\Delta P - \psi (C_f - C_p)] \tag{21}$$

$$J_s = B_s (C_f - C_p) \tag{3}$$

and $$J_s = \frac{J_w C_p}{C_{wp}} \tag{6}$$

Assuming $C_{wp} = C_w$

$$B_s (C_f - C_p)C_w = C_p A_w [\Delta P - \psi (C_f-C_p)] \tag{22}$$

$$C_f = \frac{C_p A_w \Delta P}{B_s C_w} - \frac{C_p C_f A_w \psi}{B_s C_w} + \frac{C_p^2 A_w \psi}{B_s C_w} + C_p \tag{23}$$

since $\dfrac{A_w \Delta P}{B_s} \geq \dfrac{A_w \psi}{B_s}$ and $C_f \geq C_p$

$$C_f = C_p \left[1 + \frac{A_w \Delta P}{B_s C_w} - C_p C_f \left[\frac{A_w \psi}{B_s C_w} \right] \right] \tag{24}$$

$$C_p = C_f \left[1 + \frac{A_w \Delta P}{B_s C_w} - \frac{A_w \psi C_f}{B_s C_w} \right]^{-1} \tag{25}$$

Substituting eqn. (25) in (21)

$$J_w = A_w \left[\Delta P - \psi C_f + \frac{C_f}{\left(1 + \frac{A_w \Delta P}{B_s C_w} - \frac{A_w \psi C_f}{B_s C_w} \right)} \right] \tag{26}$$

combining (1) and (26)

$$Q_p = \frac{S_a A_w}{C_w} \left[\Delta P - \Psi C_f + \frac{C_f}{\left(1 + \frac{A_w \Delta P}{B_s C_w} - \frac{A_w \psi C_f}{B_s C_w} \right)} \right] \tag{27}$$

38

let

$$\frac{S_a A_w \Delta P}{C_w} = a_1, \quad \frac{S_a A_w \psi}{C_w} = a_2, \quad 1 + \frac{A_w \Delta P}{B_s C_w} = a_3, \quad \frac{A_w \psi}{B_s C_w} = a_4 \quad V_{f_0} = a_5 (28)$$

$$\frac{dC_f}{dt} = \frac{\left[a_1 C_f - a_2 C_f^2 + \frac{a_2 C_f^2}{a_3 - a_4 C_f}\right]\left(1 - \frac{1}{a_3 - a_4 C_f}\right)}{\left(a_5 - a_1 t + a_2 C_f t - \frac{a_2 C_f t}{a_3 - a_4 C_f}\right)} \qquad (29)$$

Once C_f can be calculated at any time, permeate cone, rejection and flux can be determined using the following eqn. Eqn. (25) becomes

$$C_p = \frac{C_f}{a_3 - a_4 C_f} \qquad (30)$$

Overall mass balance

$$V_{f_0} C_{f_0} = \left[V_{f_0} - V_p\right] C_f \; V_p \; C_{pav} \qquad (31)$$

$$C_{f_0} = \left[1 - \frac{V_p}{V_{f_0}}\right] C_f + \left[\frac{V_p}{V_{f_0}}\right] C_{pav} \qquad (32)$$

Recovery is expressed in terms of C_f, C_{f_0} and C_{pav}

$$\frac{V_p}{V_{f_0}} = \frac{C_f - C_{f_0}}{C_f - C_{pav}} \qquad (33)$$

An eqn. for the total dissolved solid concentration in the product tank, C_{pav} can be obtained by substituting eqn. (30) into eqn. (12)

$$\frac{dC_{pav}}{dt} = \frac{Q_p (C_p - C_{pav})}{V_p} \qquad (34)$$

Equation (27), (30), (33) are substituted [1] in terms of C_f, C_{pav} and system constant in eqn. (34).

$$\frac{dC_{pav}}{dt} = \frac{S_a A_w}{V_{f_0}(C_f - C_{f_0})} \left[\Delta P - \psi C_f + \frac{C_f}{\left(1 + \frac{A_w \Delta P}{B_s C_w} - \frac{A_w \psi C_f}{B_s C_w} \right)} \right] x$$

$$\left[\frac{C_f}{a_3 - a_4 C_f} - C_{pav} \right] x \ (C_f - C_{pav}) \hspace{3cm} (35)$$

Eqn. (29) and (35) are solved simultaneously using fourth order R-K method (12).

4.2 ESTIMATION OF PARAMETERS

The solvent permeability constant A_w was determined by operating the experimental system at different pressure using distilled water as the feed. For distilled water $\pi_f = 0$, $J_w = A_w \Delta P$. The solute permeability constant was determined by operating the system at several different concentration of the feed at constant pressure. Since $J_s = B_s \Delta C$ and $\frac{J_w C_p}{C_w} = B_s \ (C_f - C_p)$ yields B_s.

During the RO run for the determination of B_s, the pressure can be varied. Since A_w is previously found for pure water, the relationship

$[\Delta P - (J_w/A_w)] = \psi \ (C_f - C_p)$ is used to determine ψ (12).

CHAPTER V

RESULT AND DISCUSSION

This chapter describes the results obtained in respect of the following:

- Estimation of parameters

- Numerical Simulation of Experiments

- Characteristics of membranes, prepared in the laboratory.

The flow rate fluctuations are main cause of discrepancies in the results obtained. However, all possible efforts have been made to control it; but fluctuations were still there. The flow rate fluctuations will effect permeate concentration, retentate concentration and permeate flow rate. The flow rates were computed using the material balance for salt, and the figure 5.1 shows the fluctuations. This correspond to the initial feed concentrations of 0.2% to 0.8%. The measured flow rates vary from 14.1 to 13 litre/min, and are calculated by collecting a definite volume in tank and measuring the time with stop watch. The flow rate is assumed to be constant in numerical simulation of experiments for each set of experimental data.

5.1 ESTIMATION OF PARAMETERS

The parameters, solvent permeability constant, solute permeability constant, and osmotic pressure to solute concentration ratio are important parameters, required in numerical simulation. The value of these parameter is calculated from the experimental data using least square method. The equations used for the calculations are presented in the previous Chapter.

5.1.1 Solvent permeability constant

The experimental observations for the calculation of solvent permeability constant are shown in Appendix D (Table D.2). The value of solvent permeability constant thus calculated is, A_w = 9.86 x 10^{12} hr/m. The experimental result and theoritical values of solvent flux are compared and shown in Fig.5.2. The values are found within ± 5% deviation.

5.1.2 Solute permeability constant

The experimental observations for the calculation of solute permeability constant are presented in Appendix B. The calculated value of solute permeability constant is, B_s = 5.66 x 10^{-4} m/hr. The values of experimental and theoritical solute fluxes are compared and found within ± 5% deviation. The comparison is shown in Fig.5.3.

5.1.3 Osmotic pressure to solute concentration ratio

The experimental observations for the calculation of osmotic pressure to solute concentration ratio are shown in Appendix D (Table D.1). The value of the osmotic pressure to solute concentration ratio determined is, ψ = 1.91 x 10^{12} m^2/hr^2. The experimental and theoritical values are compared and found to vary within ± 10% range. The comparison is shown in Fig.5.4. The calculation for osmotic pressure to solute concentration ratio involves the value of solvent permeability constant also; due to this reason percent deviation has increased to 10%.

5.2 NUMERICAL SIMULATION OF EXPERIMENTS

The mathematical model given in Chaper IV was validated for the RO system operating in the semi-batch, unsteady mode of operation. Solution-diffusion models were utilized to depict mass transfer to the membrane. The mass transfer constant

for these models were determined experimentally. System material balances, together with these mass-transfer models were used to simulate system operation. Correlation of flux, solute concentration, feed concentration and rejection with operating time are functions of the model.

Six model constants and two initial conditions were used in the simulation programme. The initial conditions are feed concentration, C_{f0}, and feed volume V_{f0}. Membrane surface area, S_a and operating pressure gradient ΔP are two model constants that represent design variables. The solvent or water concentration is denoted by C_w. Three other constants for the solution diffusion equation were determined experimentally using simple steady state operating runs on the RO system. The constants are given as follows:

$$C_w = 1.0 \times 10^3 \text{ kg/m}^3$$

$$\Delta P = 1.9 \times 10^{13} \text{ kg/m} \times \text{hr}^2$$

$$S_a = 0.302 \text{ m}^2$$

Experimental results and simulated values are compared for initial feed concentration varying from 0.2% to 0.8%. The compared values are feed concentration, permeate concentration, solvent flux and rejection. The experimental observations are shown in Appendix B.

5.2.1 Feed concentration

Figure 5.5 presents the curves of feed concentration with time, observed experimentally as well as predicted by the model. Although the predictions are lower than the experimental ones, but the deviation is acceptable. Similar observations can also be made from Figures 5.9, 5.13 & 5.17. The desired values are not obtained experimentally because of the following reasons:

(i)   **Calibration:** The conductivity is measured for the salt concentration in feed permeate, and retentate. The calibration is done by making different solutions of salt concentration. These solutions are taken for calibration from 0.1 to 1.2%. The calibration curve is given in Appendix A. The correlation is given below:

$$y = 0.0641x - 0.0094, \quad R^2 = 0.9957$$

where x = conductivity of solution, mmho

         y = percent salt concentration

The concentration is calculated from the calibration between percent salt solution and conductivity.

(ii)   **Pressure measurement:** Though pressure was fluctuating, but it is assumed to be constant for all the experimental data.

(iii)   **Volume measurement:** Feed volume is measured by collecting a definite volume in tank and measuring the time. Permeate flow rate is also measured using flask and stop watch. These measurements are likely to be erroneous.

(iv)   **Fouling of membrane:** This is responsible for concentration polarization, and it is not taken into consideration in numerical simulation.

(v)   **Mixing:** There is no proper mixing in feed tank.

5.2.2 Permeate concentration

In unsteady state mode of operation retentate is recycle to the feed tank, its concentration is always incrementally greater than feed concentration. Because of permeate production the feed volume continuously decreases in the tank, so feed concentration increases. The permeate concentration increases due to increase in concentration driving force as shown in figure 5.6. Similar observations can also be made from figures 5.10, 5.14 and 5.18.

5.2.3 Solvent flux

The simulation suggests that the solvent flux decreases continuously with time. Initially the feed volume in tank is large, the flux decreases slowly at first and when concentration gradient increases the flux falls sharply as shown in Fig.5.7. This behaviour is in accordance with the observations made in the literature (12), however, the values of experimental and simulated values differ within acceptable limit because of reasons mentioned above. Similar behaviour is also shown for other experimental runs shown in figure 5.11, 5.15, and 5.19.

5.2.4 Percent salt rejection

Percent rejection is based upon the permeate concentration. As simulation gives lower value of permeate concentration, rejection is more for simulated value. Practically permeate concentration is more so separation is less. The experimental value of percent salt rejection is always lesser than the simulated value as shown in Figures 5.8, 5.12, 5.16 and 5.20.

5.2.5 Computational aspects:

As described earlier, simplified model has been solved by using the computational algorithm, developed on the basis of fourth order Runge Kutta Method. The algorithm is programmed in C++ and excuted on a PC Busybee XL, 486 GA/66.

After conducting several numerical experiments, it has been found that a step size of 5 min. in time is appropriate for solving the model, which is also the time interval taken for the experimental data.

5.3 CHARACTERISTICS OF MEMBRANES, PREPARED IN THE LABORATORY

Scatter electron microscopy was used for structural analysis of cellulose acetate and cellulose acetate aided with magnisium chloride, membrane. The

photographs have been taken and are shown in Fig.5.21 to 5.25. It is evident from the picture that magnesium chloride membrane gives irregular pores as shown in Fig.5.21 and 5.22. The cellulose acetate membranes have uniform pore distribution and are shown in Fig.5.23 and 5.24. In some cellulose acetate membranes, pores are not visible that means pore size is very small as shown in Fig.5.25.
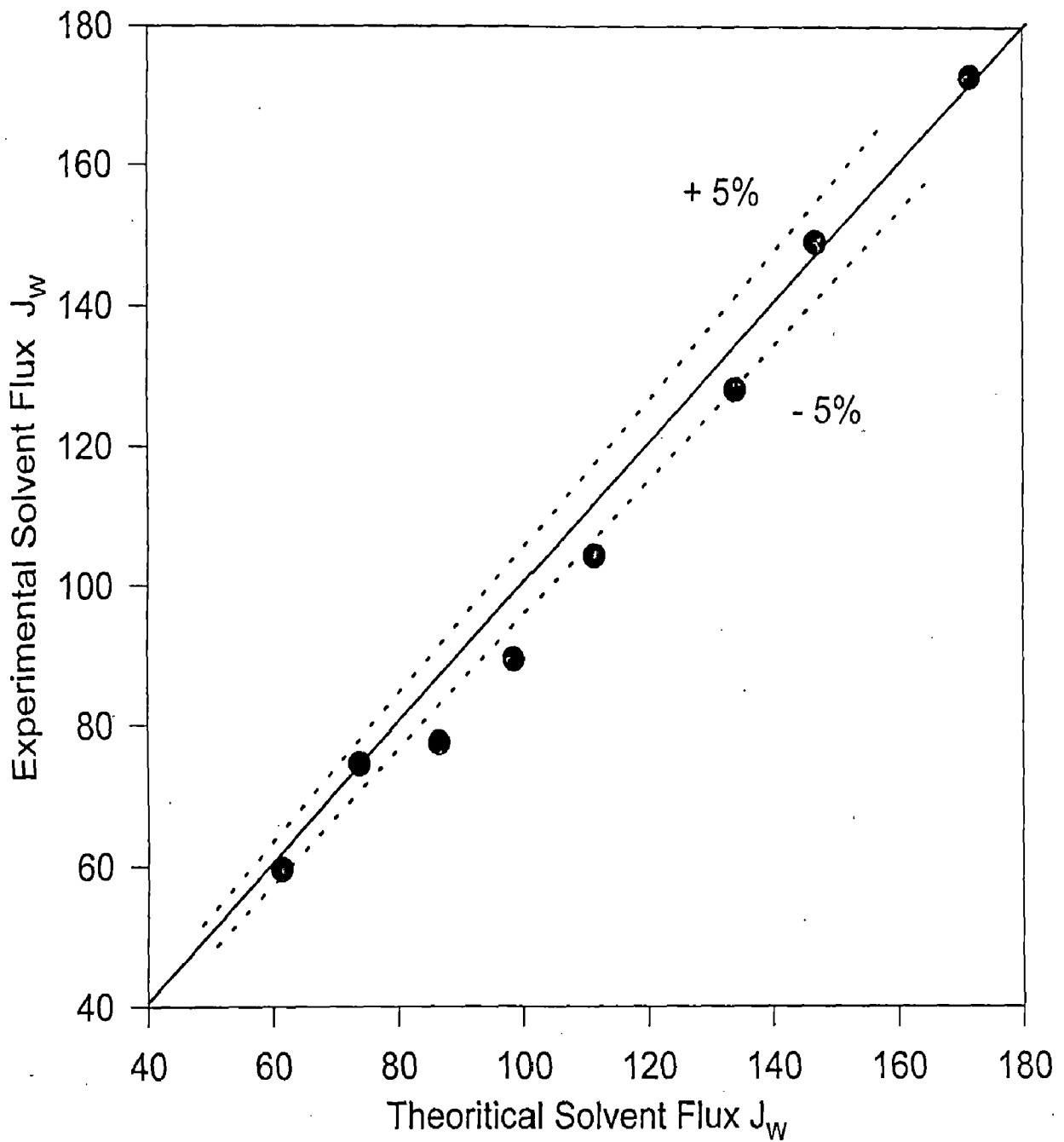
Fig. 5.2 Comparison of experimental and theoritical solvent flux, i.e. $jw_{exp} = (Q_p/S_a)*C_{wp}$ and $jw_{th} = A_w*del\ P$.
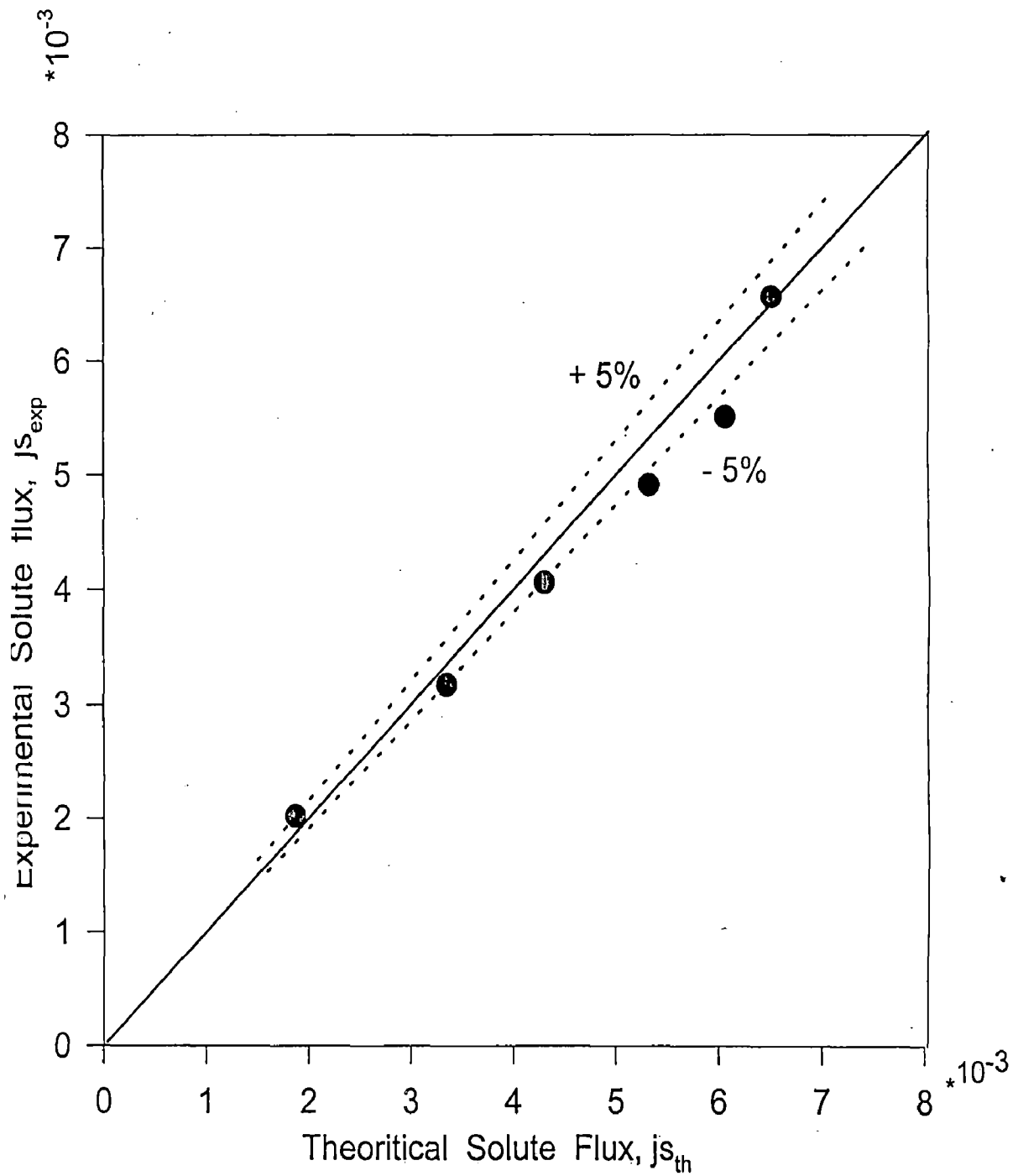
Fig. 5.3 Comparison of Experimental Solute Flux and theoritical Solute Flux, i.e. $js_{exp} = (j_w{}^*C_p) / C_w$ and $js_{th} = B_s{}^*(C_f - C_p)$.
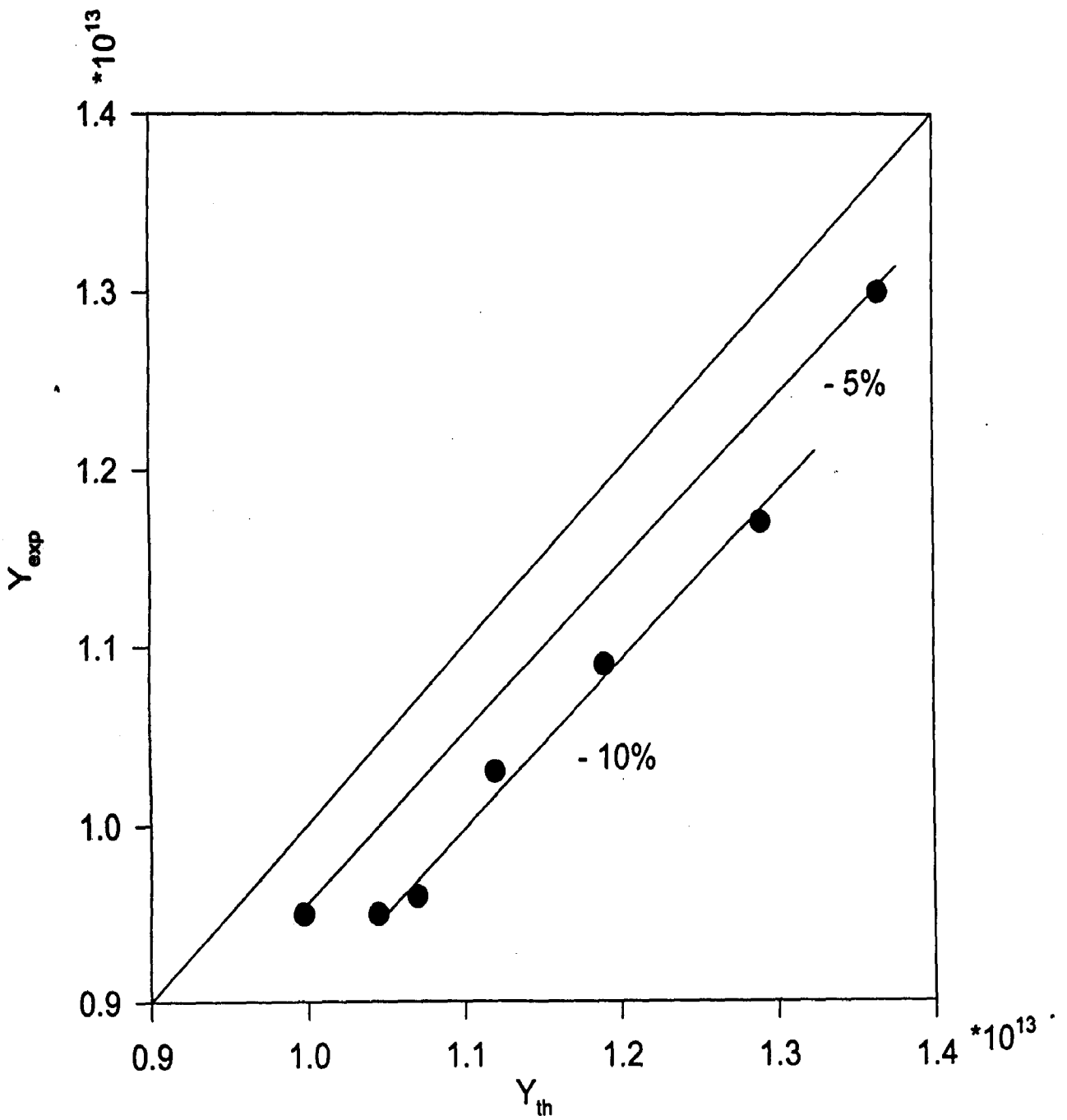
Fig. 5.4 Comparison of experimental and theoritical value
using the relationship, [del P-(J_w/A_w)] = psi*(C_f-C_p).

G 10,167

50
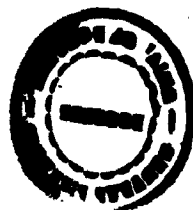
Fig. 5.5 Comparison of experimental and simulated values
of feed concentration at different times.
[For initial feed concentration = 0.2% of NaCl]

Fig. 5.6 Comparison of experimental and simulated values
of permeate concentration at different times.
[For initial feed concentration = 0.2% of NaCl]

Fig. 5.7 Comparison of experimental and simulated values
of solvent flux at different times.
[For initial feed concentration = 0.2% of NaCl]

Fig. 5.8 Comparison of experimental and simulated values
of percent salt rejection at different times.
[For initial feed concentration = 0.2% of NaCl]

Fig. 5.9 Comparison of experimental and simulated values
of feed concentration at different times.
[For initial feed concentration = 0.4% of NaCl]

Fig. 5.10 Comparison of experimental and simulated values
of permeate concentration at different times.
[For initial feed concentration = 0.4% of NaCl]
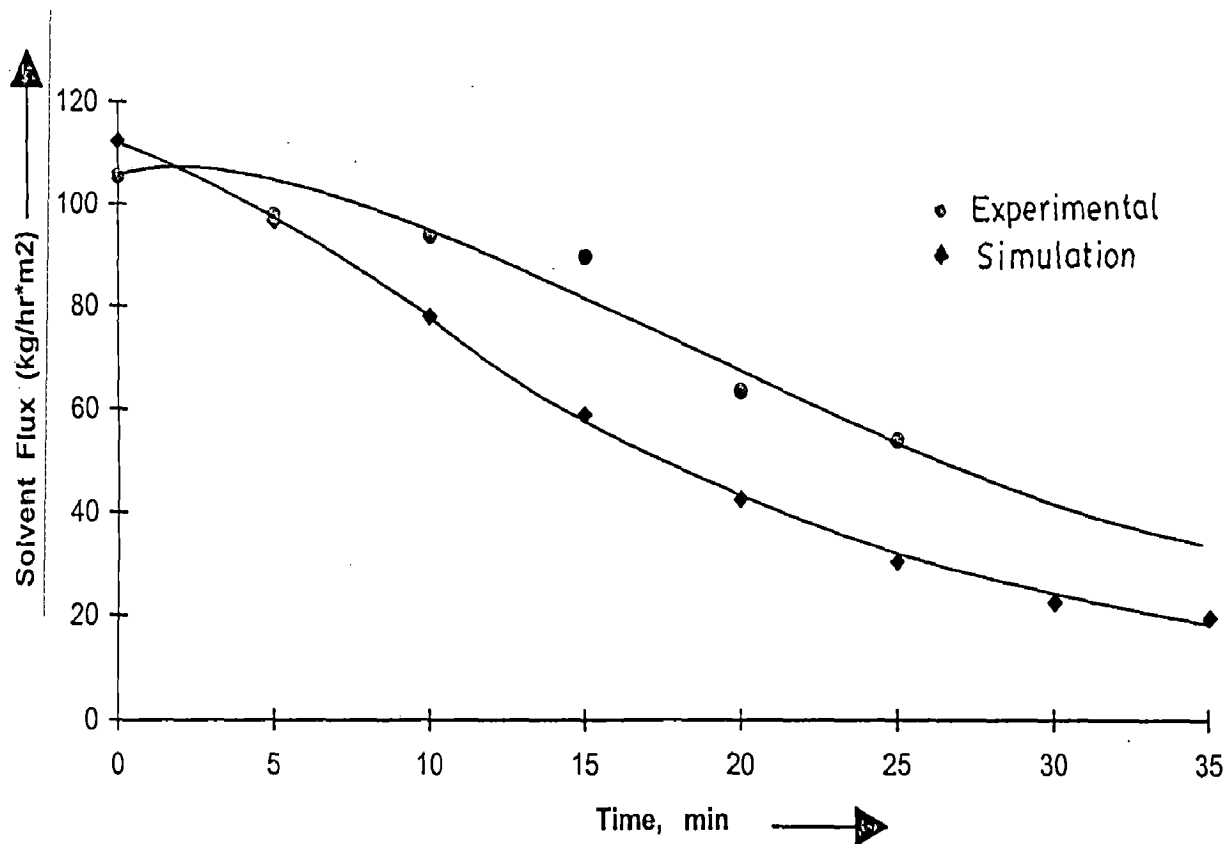
Fig. 5.11 Comparison of experimental and simulated values
of solvent flux at different times.
[For initial feed concentration = 0.4% of NaCl]
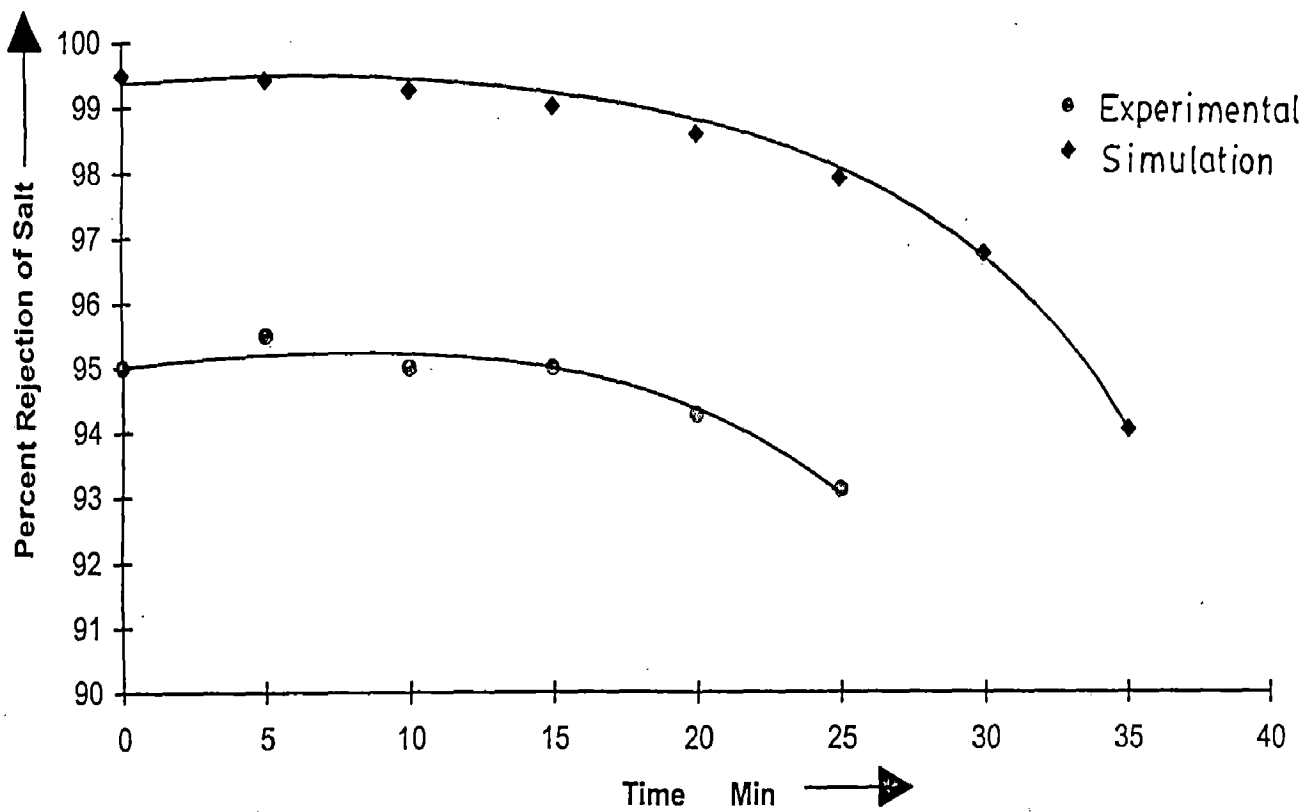
Fig. 5.12 Comparison of experimental and simulated values
of percent salt rejection at different times.
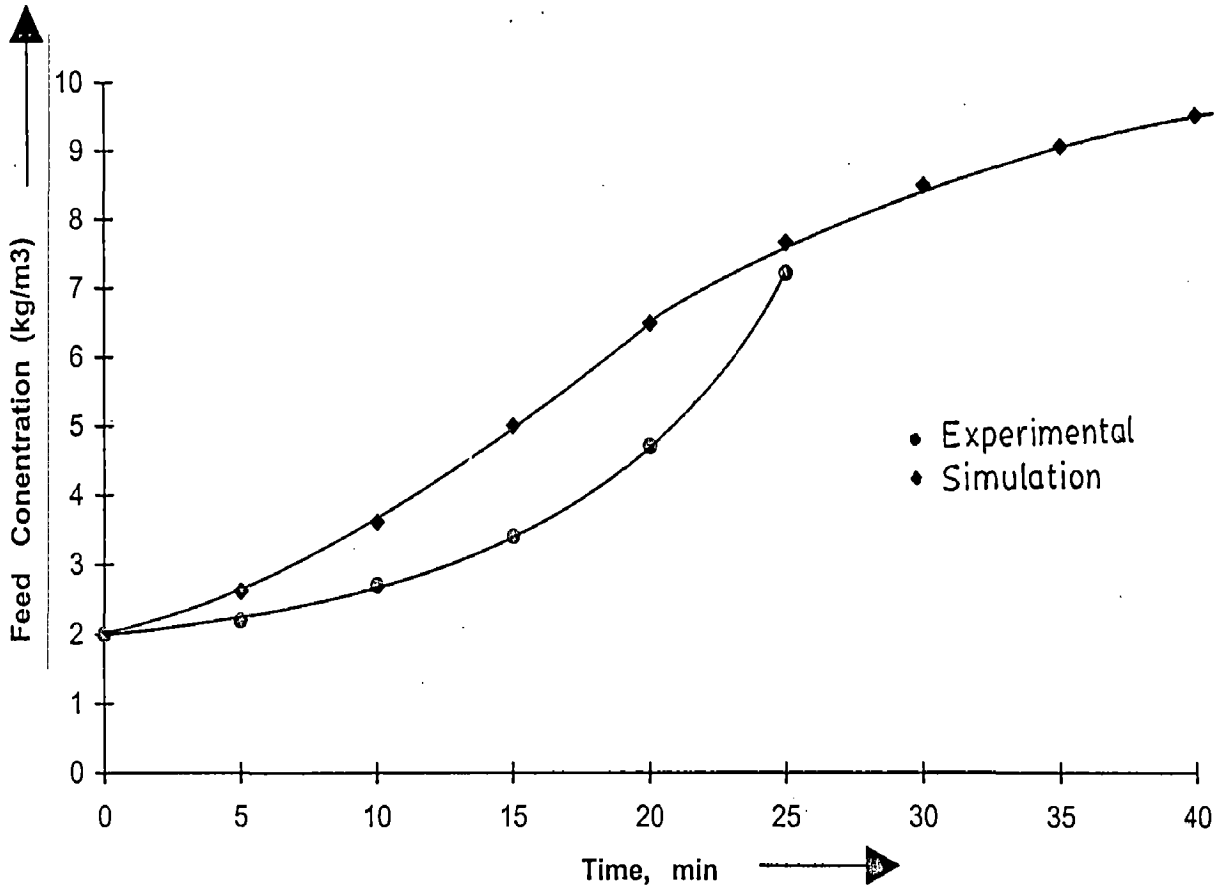[For initial feed concentration = 0.4% of NaCl]
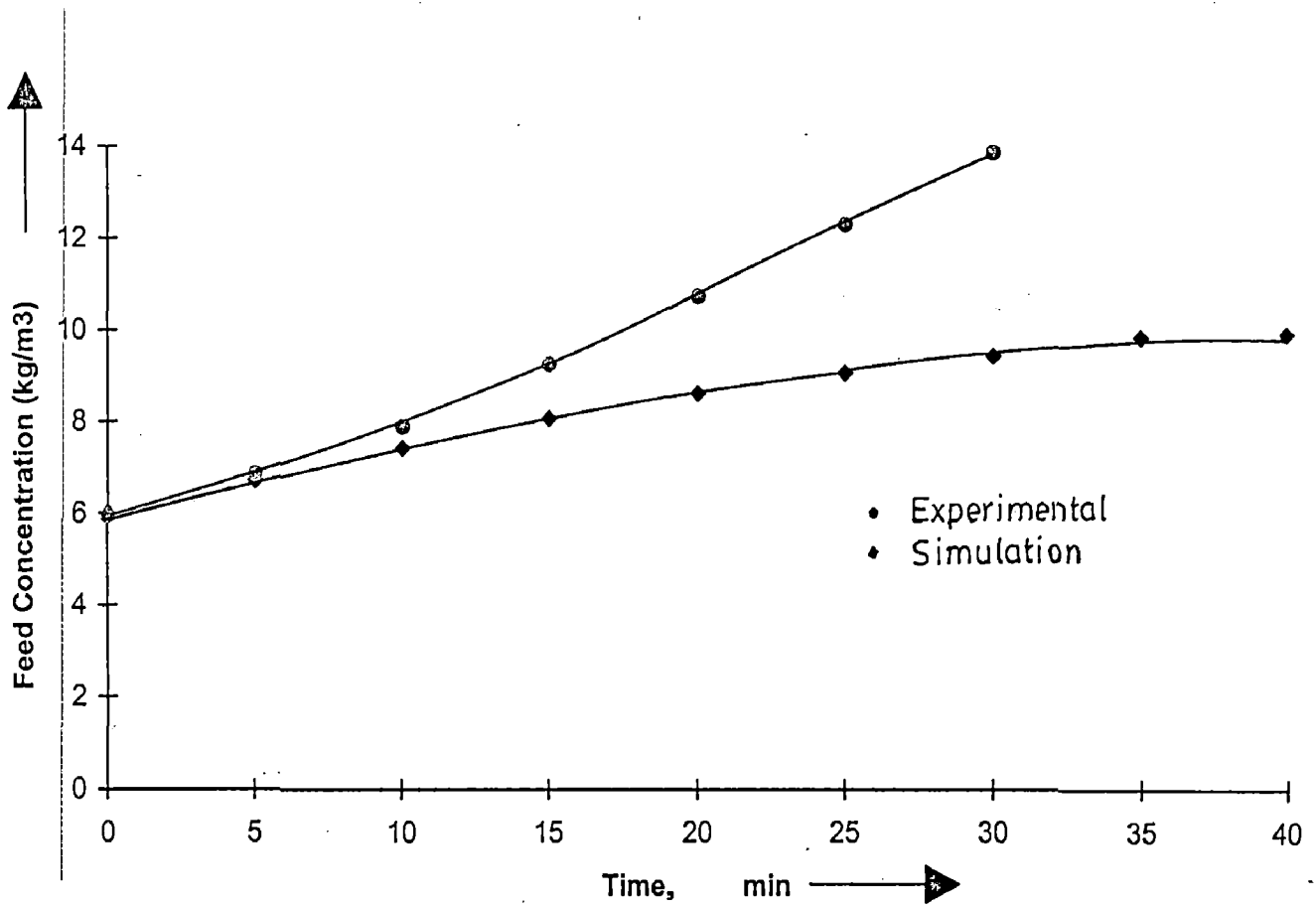
Fig. 5.13 Comparison of experimental and simulated values
of feed concentration at different times.
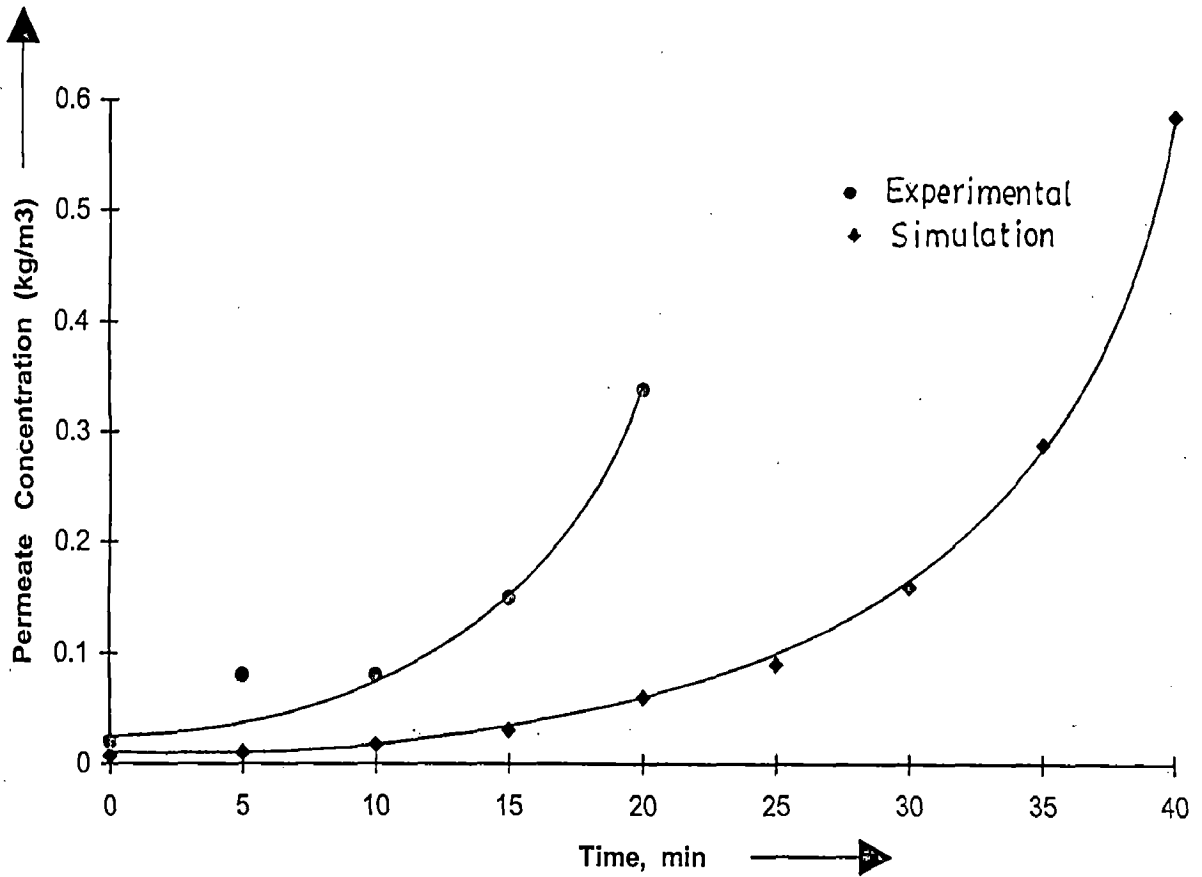[For initial feed concentration = 0.6% of NaCl]
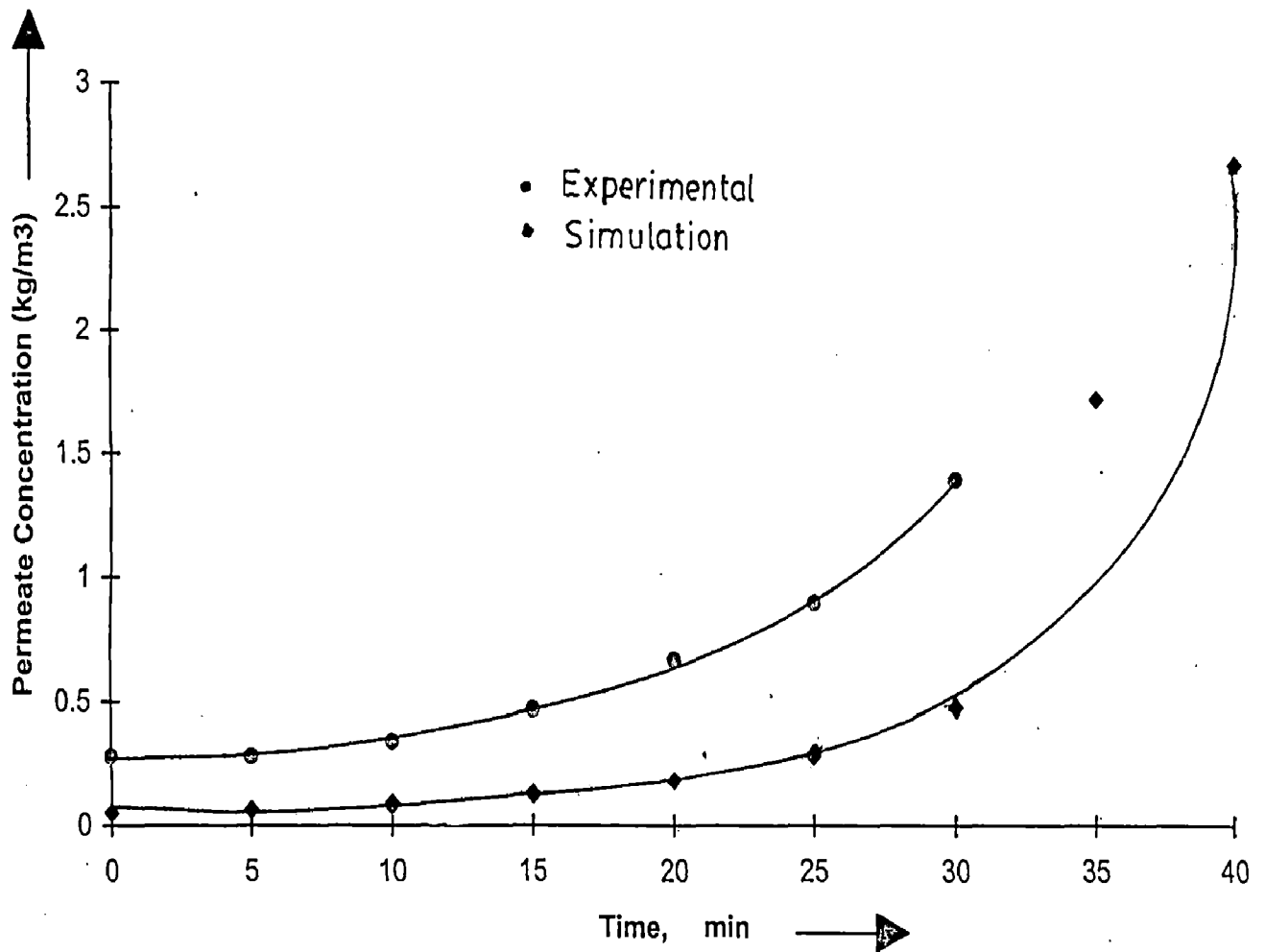
Fig. 5.14 Comparison of experimental and simulated values
of permeate concentration at different times.
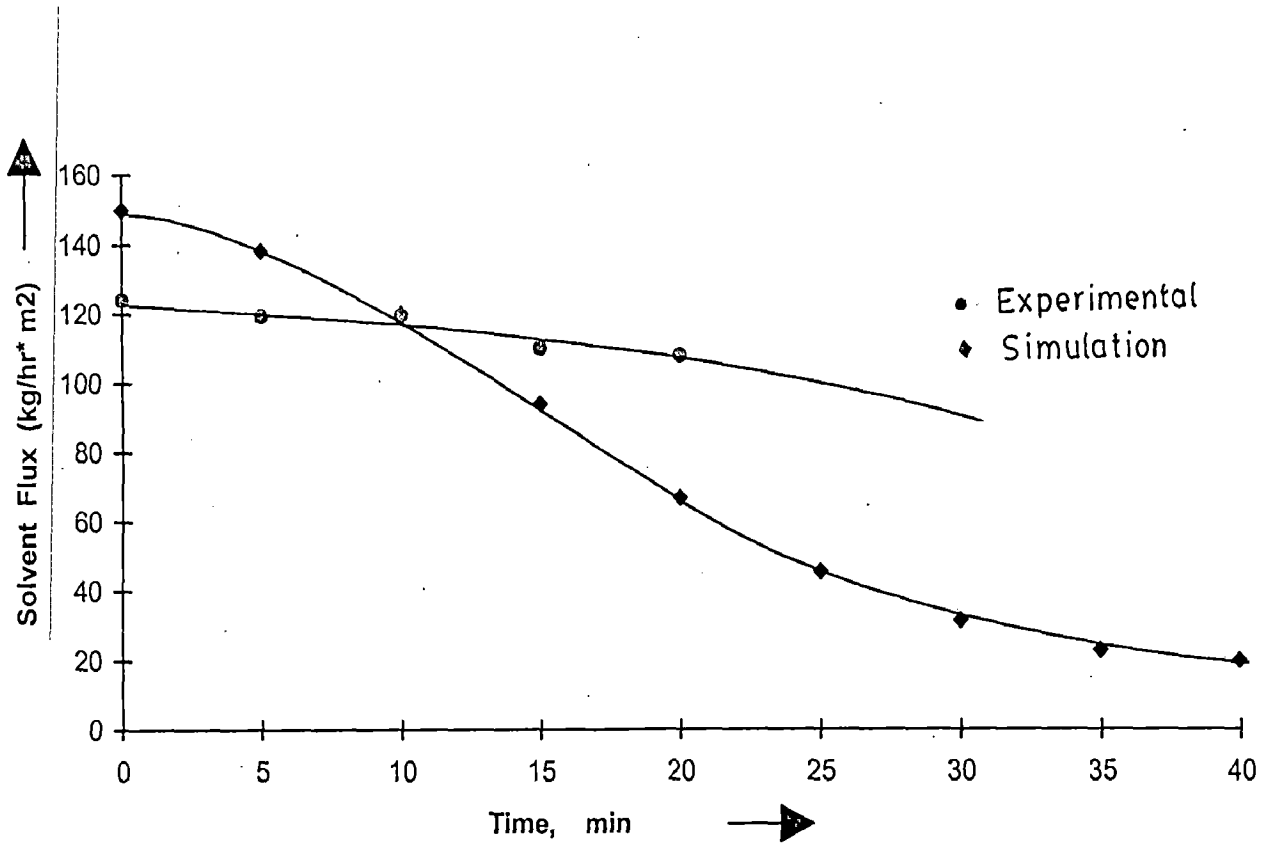[For initial feed concentration = 0.6% of NaCl]
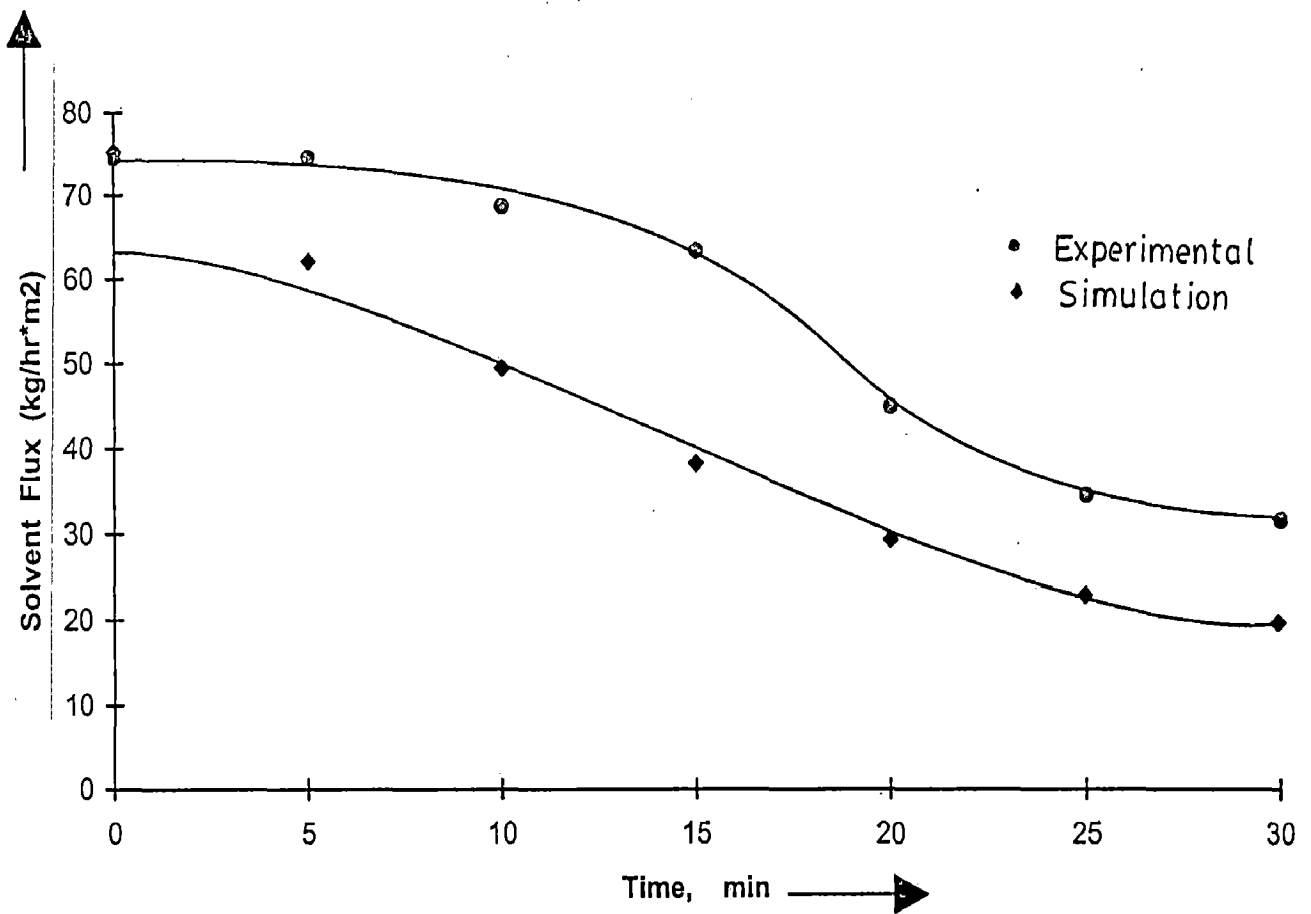
Fig. 5.15 Comparison of experimental and simulated values
of solvent flux at different times.
[For initial feed concentration = 0.6% of NaCl]
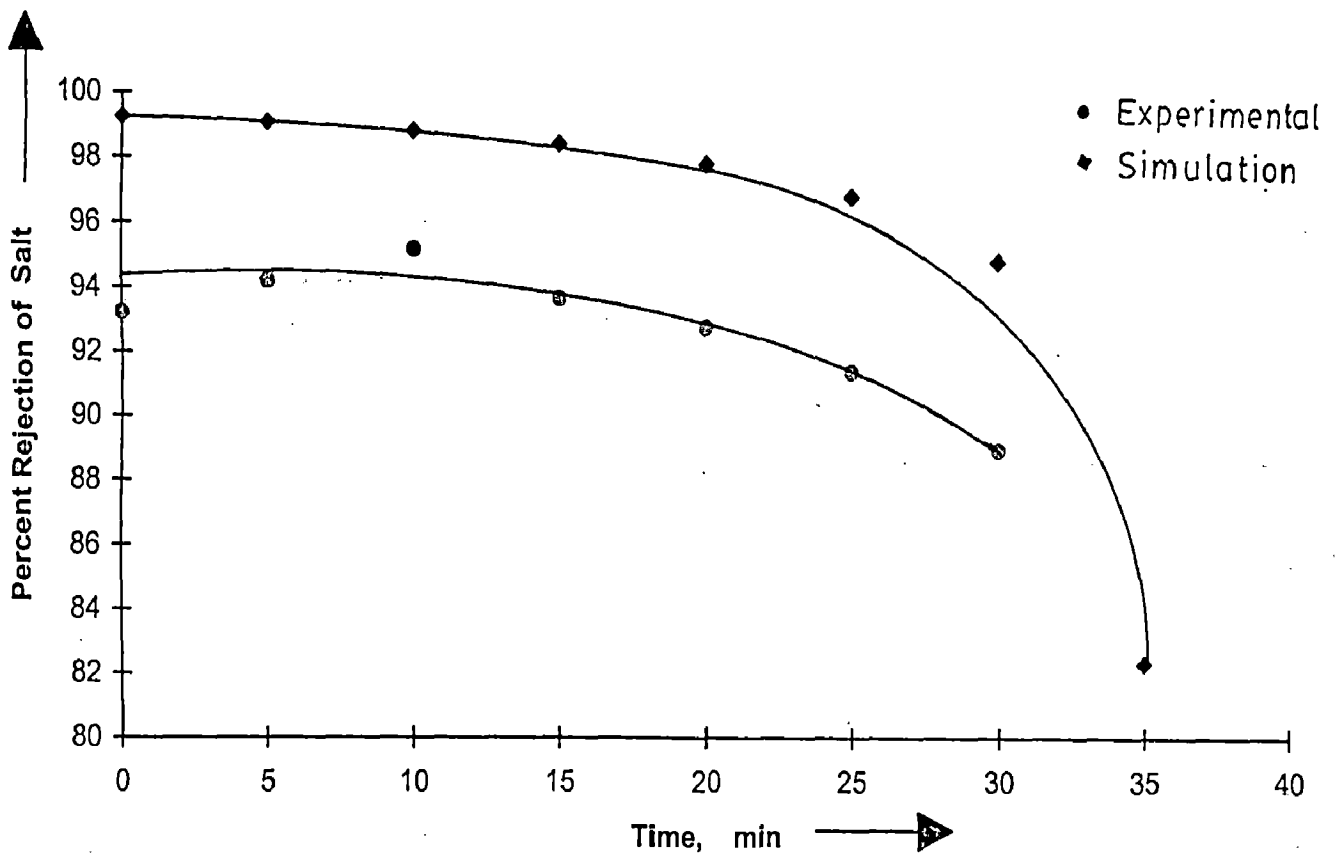
Fig. 5.16 Comparison of experimental and simulated values
of percent salt rejection at different times.
[For initial feed concentration = 0.6% of NaCl]

62
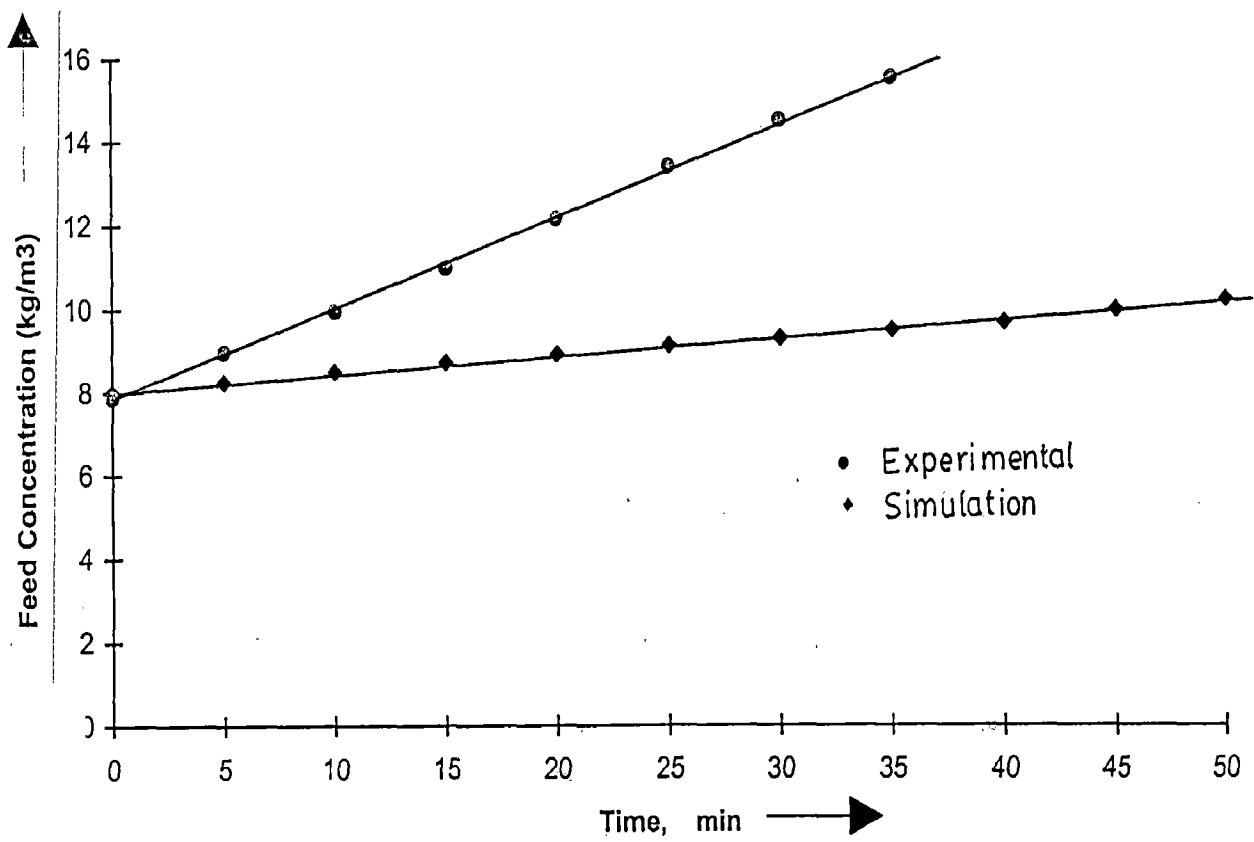
Fig. 5.17 Comparison of experimental and simulated values
of feed concentration at different times.
[For initial feed concentration = 0.8% of NaCl]
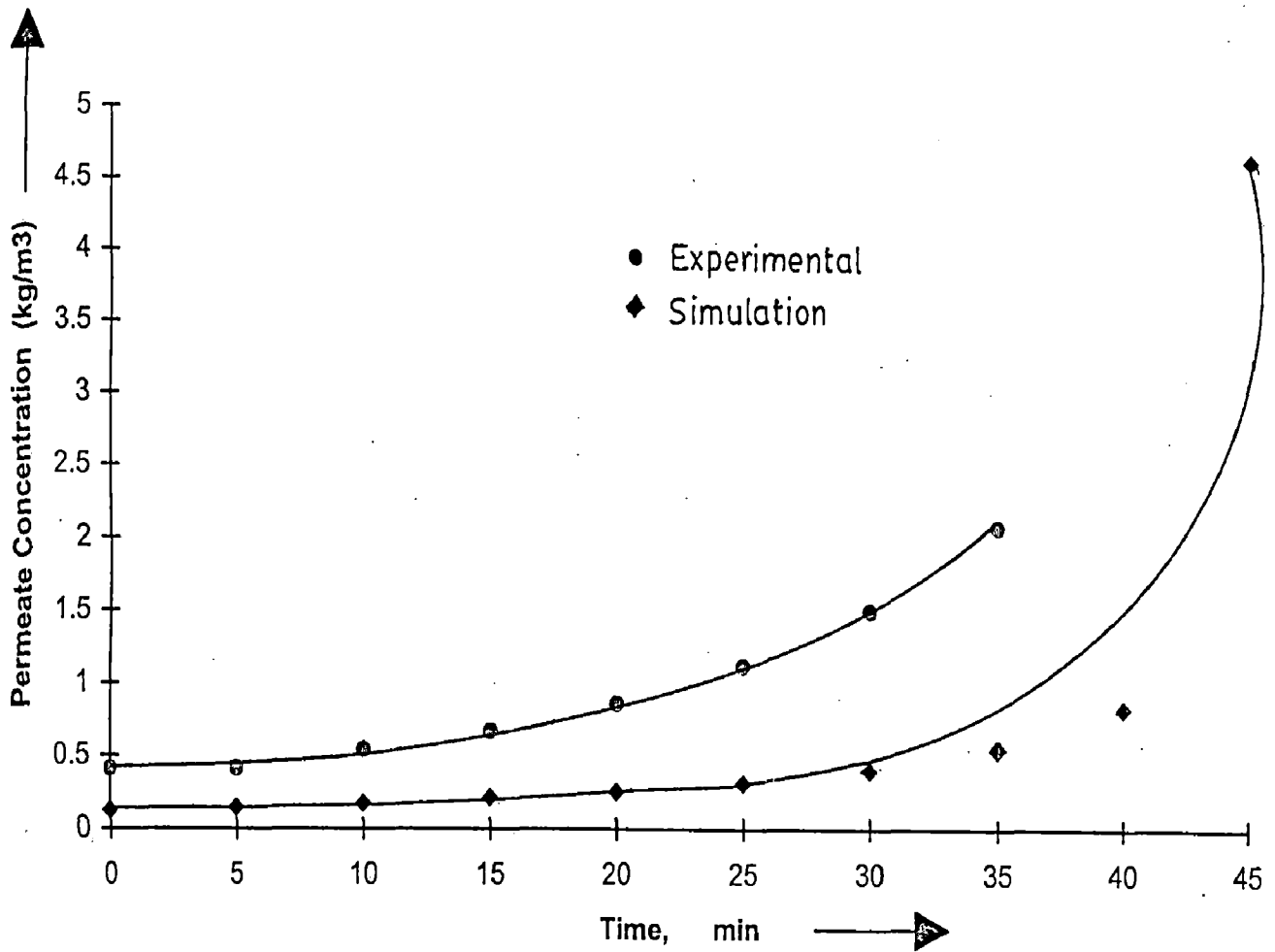
Fig. 5.18 Comparison of experimental and simulated values
of permeate concentration at different times.
[For initial feed concentration = 0.8% of NaCl]
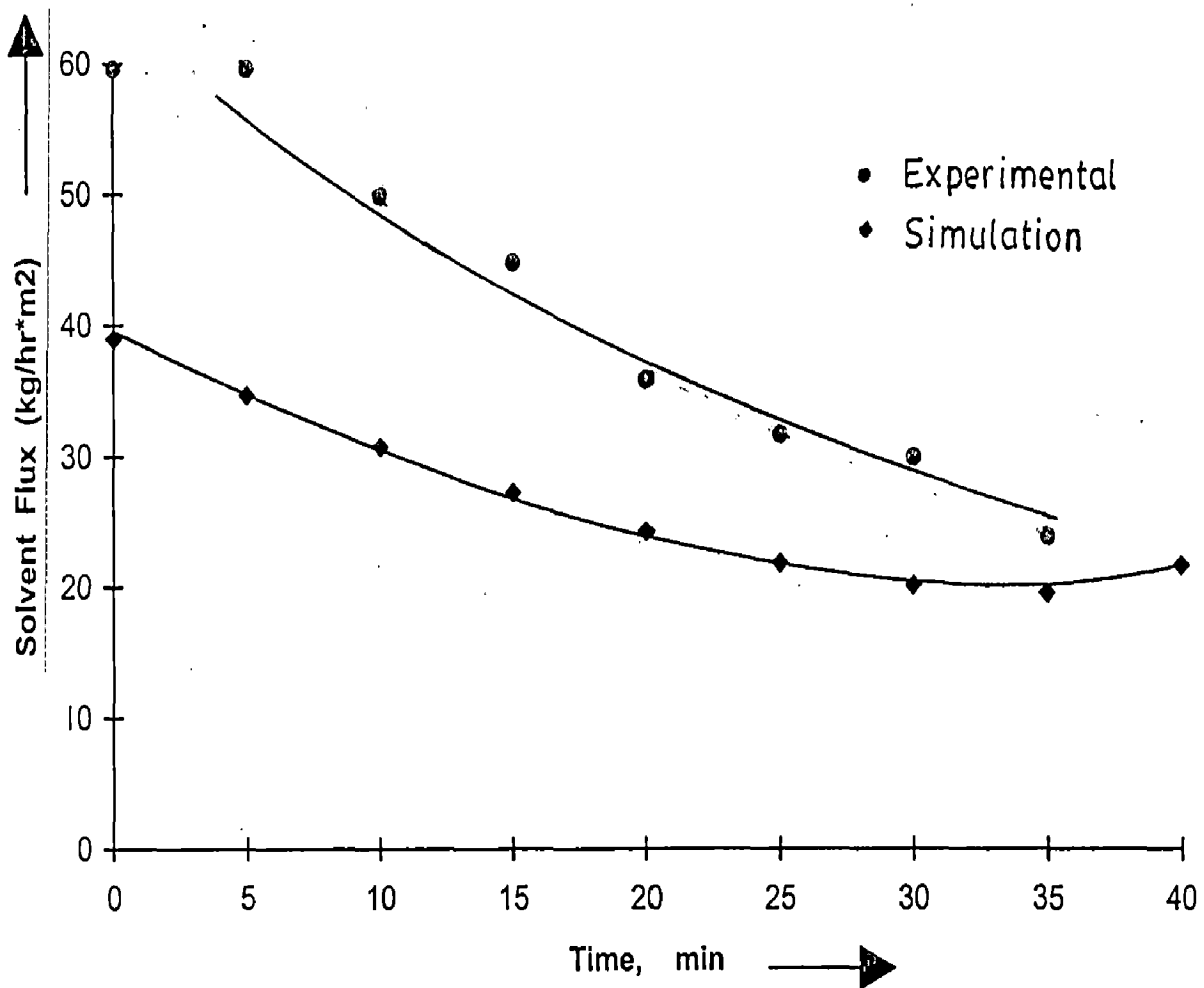
Fig. 5.19 Comparison of experimental and simulated values
of solvent flux at different times.
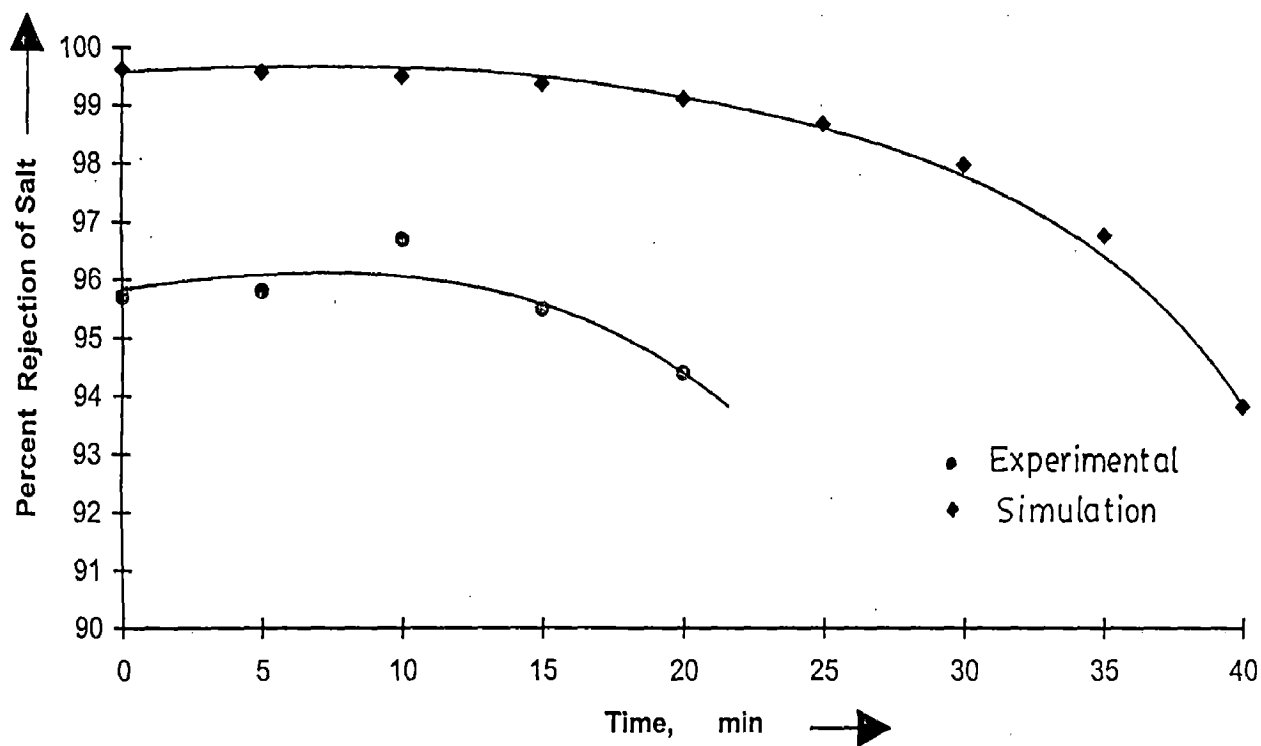[For initial feed concentration = 0.8% of NaCl]

6 5
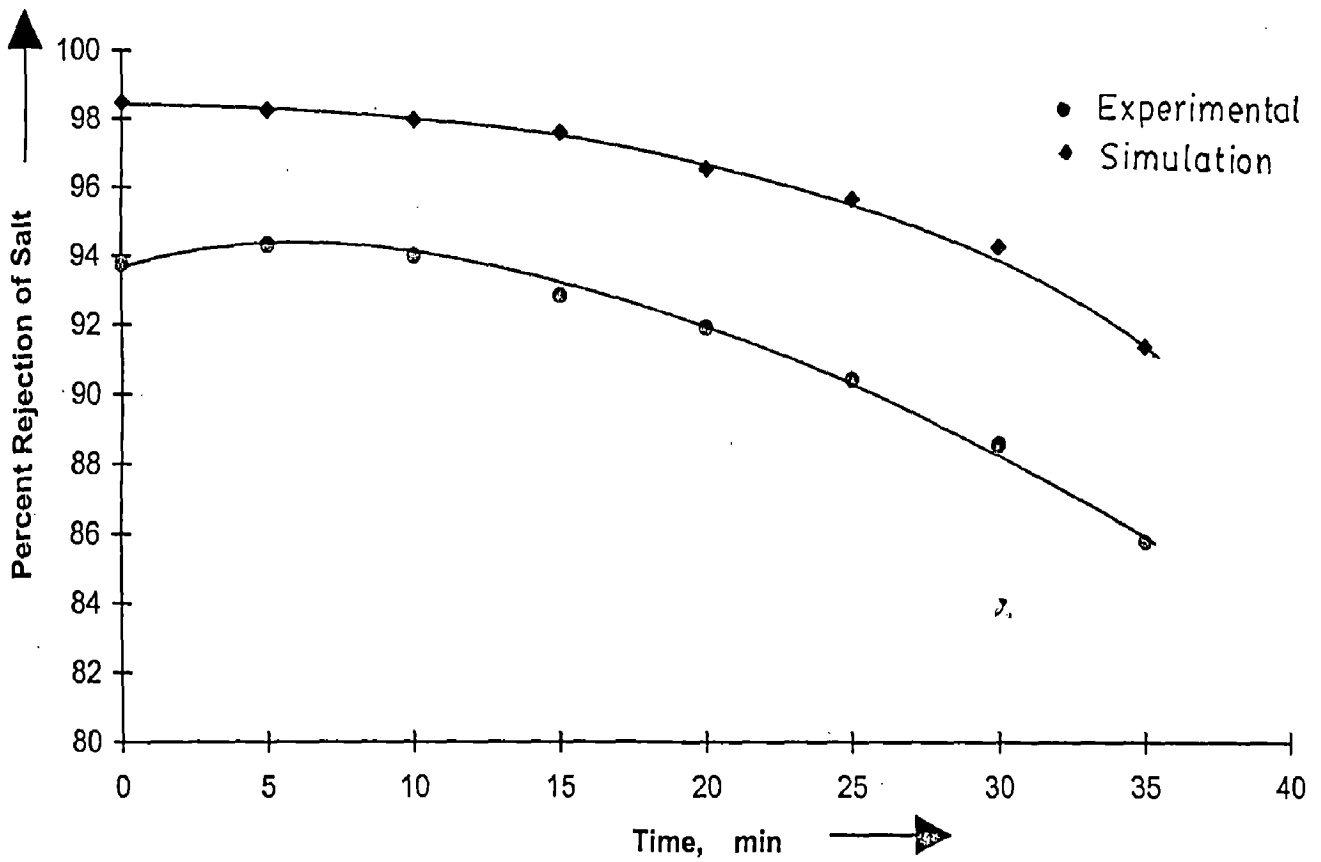
Fig. 5.20 Comparison of experimental and simulated values
of percent salt rejection at different times.
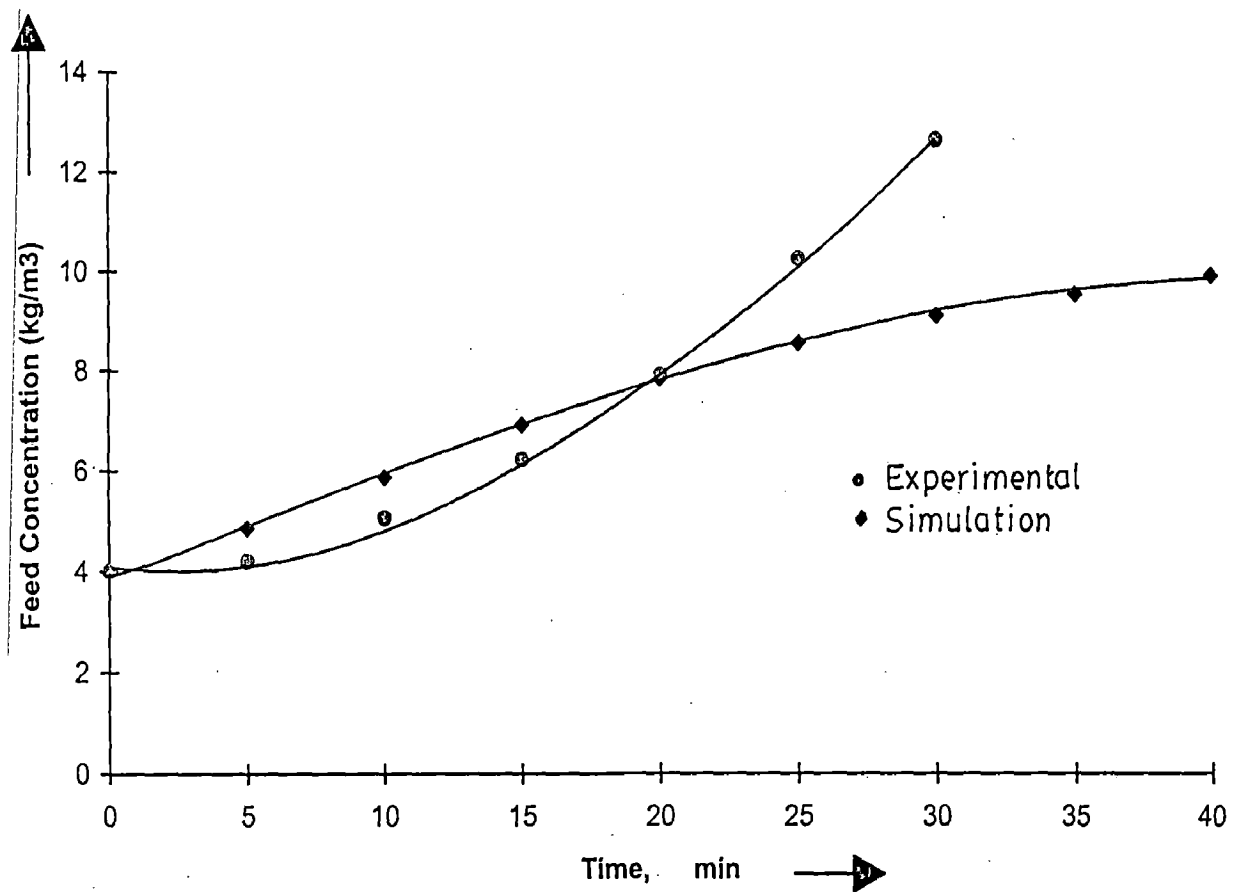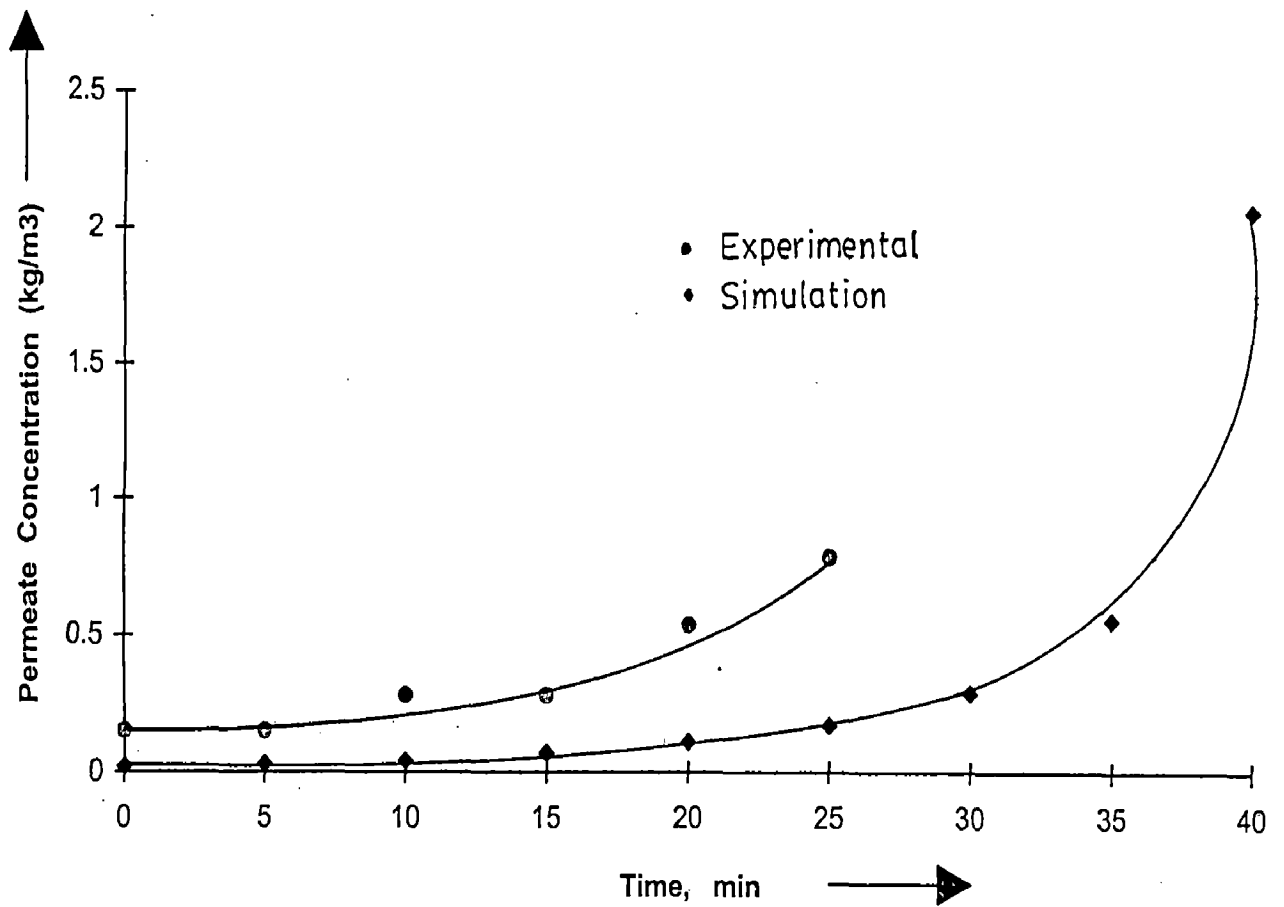[For initial feed concentration = 0.8% of NaCl]
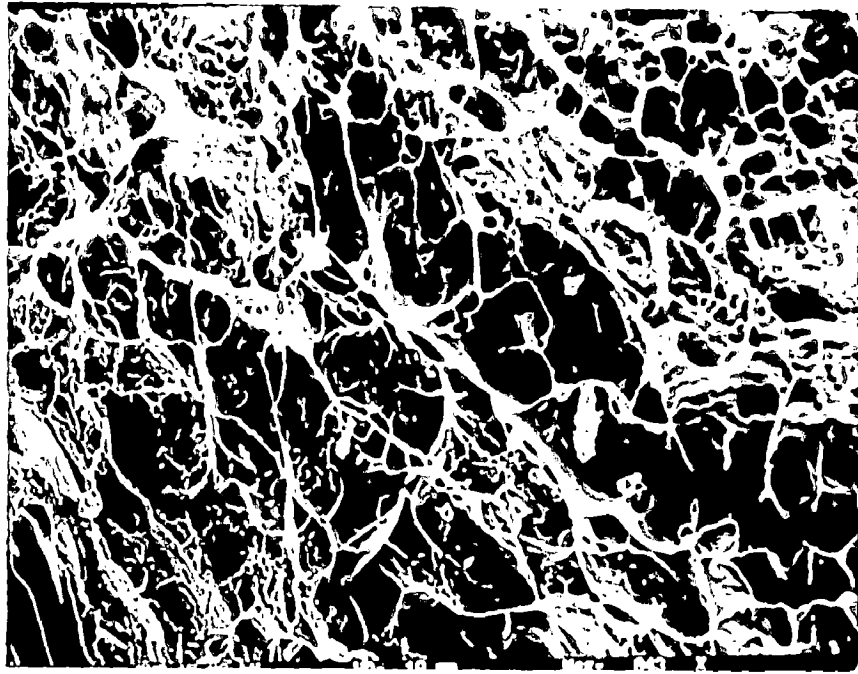
Fig. 5.21 Photograph showing cellulose acetate membrane
with megnisium chloride
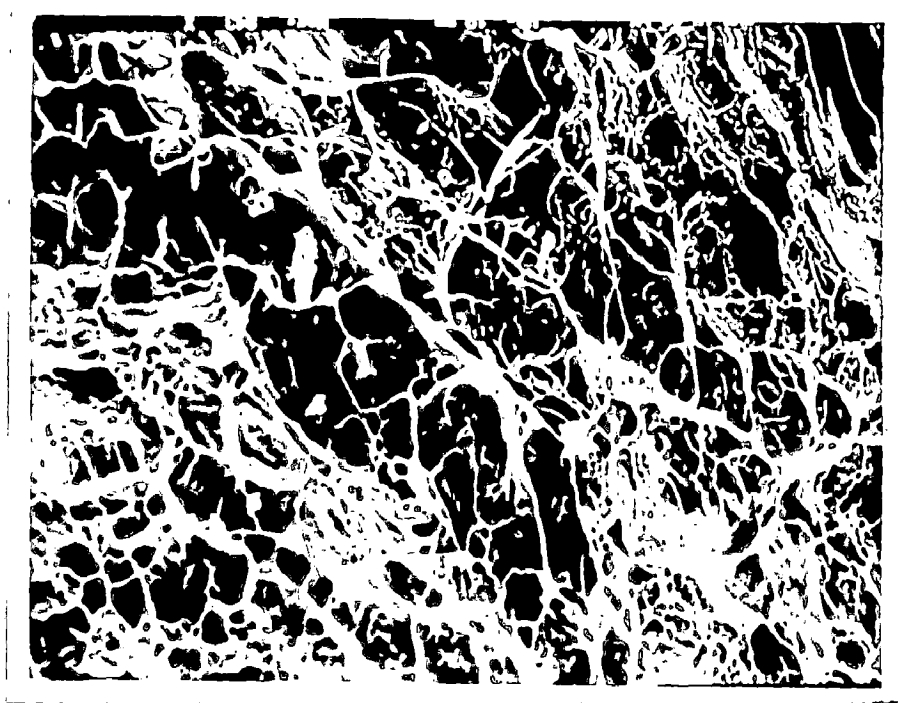
Fig. 5.22 Photograph showing cellulose acetate membrane
with megnisium chloride
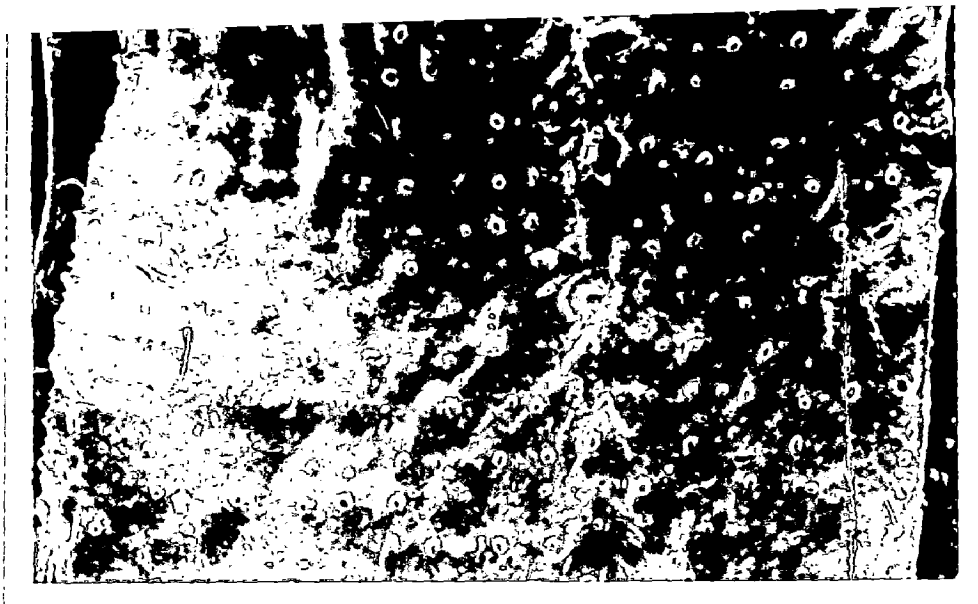
Fig. 5.23 Photograph showing cellulose acetate membrane
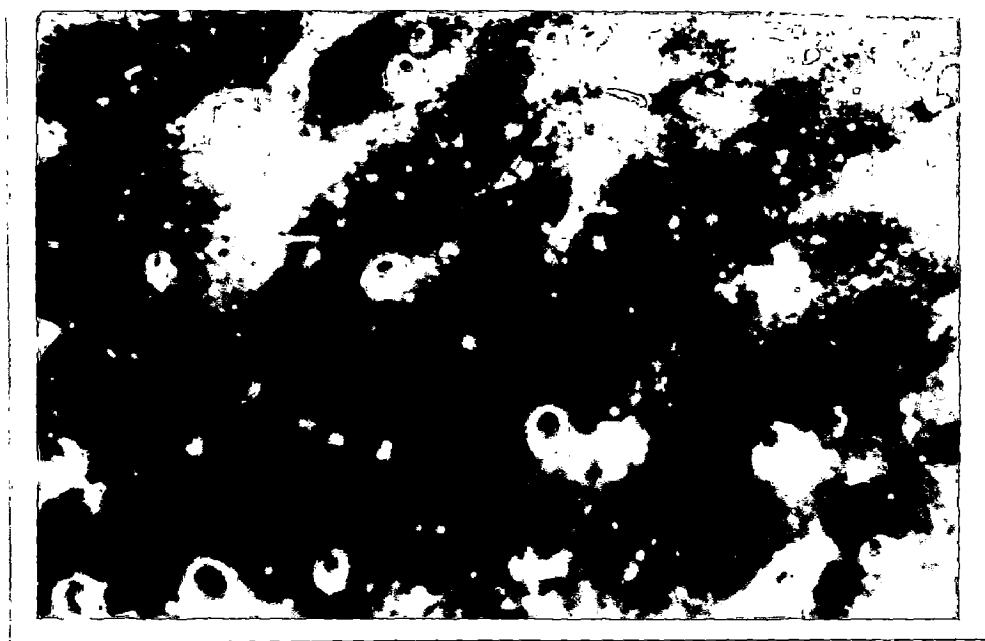
Fig. 5.24 Photograph showing cellulose acetate membrane
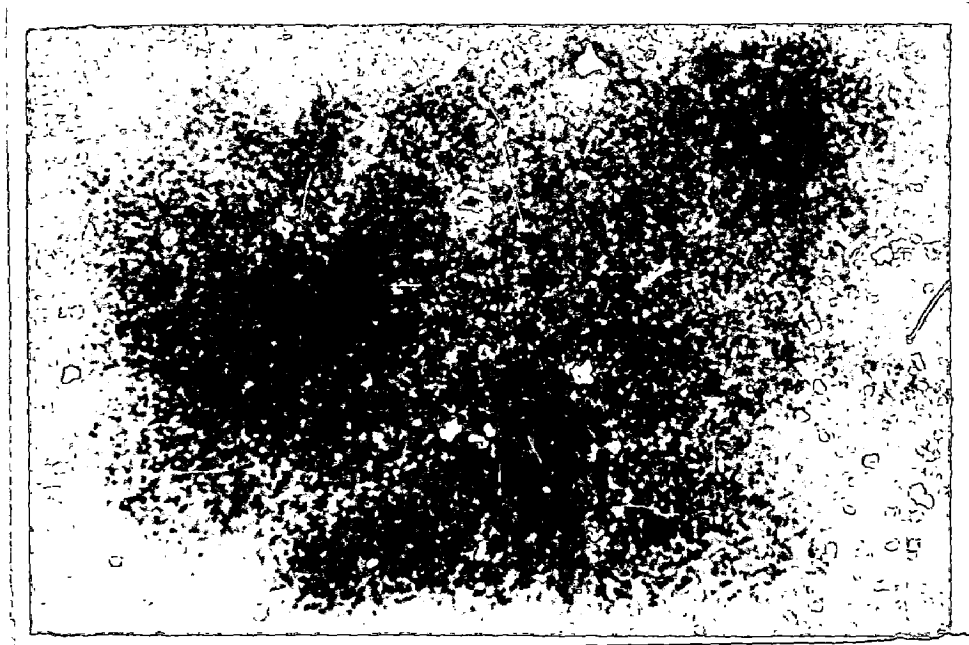
Fig. 5.25 Photograph showing cellulose acetate membrane

CONCLUSIONS AND RECOMMENDATIONS

6.1 CONCLUSIONS

As mentioned in the Chapter I on Introduction, the main objective of this dissertation is to evaluate the efficacy of experimental unit in implementing the RO process. Following conclusions are drawn on the basis of results given in previous Chapter.

(i)   Although every possible effort has been mdae to maintain the constant feed flow rate, but it varried significantly as has been seen on the basis of overall material balance (please refer to figure 5.1).

(ii)   Characteristic parameters constants have been estimated for polyamide membrane used in spiral wound module in RO process, and are given below

Solvent Permeability Constant, A_w = 9.86 x 10^{-12} hr/m

Solute Permeability Constant, B_s = 5.66 x 10^{-4} m/hr

$$\Psi = 1.91 \times 10^{12} \ m^2/hr^2$$

Variations between experimental and predicted values of solvent flux, solute flux, and $\Delta P - (J_w/A_w)$ using above estimated constants remained between 5-10%. Thus, the estimate of constants may be assumed to be accurate. Further, the order of magnitudes of constants compares well with these reported in the literature (12).

(iii)   Numerical simulation of experiments shows that the simulated and experimental observation show the same behaviour/qualitatively. However, their magnitude differs. This is due to the variation in feed flow rate, while it is presumed to be constant during an experimental run.

69

On the basis of above, it is summarized that the experimental unit is capable of demonstrating RO process qualitatively. However, it requires modification in respect of constancy of feed flow rate and its measurement. Then it would be able to provide reliable and accurate experimental observation.

Further, membranes are prepared in the laboratory. Its SEM analysis emphasizes the need of membrane development under directly controlled conditions as is evident from the SEM photographs depicting varied permeability/porosity.

6.2 RECOMMENDATIONS

(i)   In order to damp the variations in feed flow rate, an intermediate tank between feed pump and RO module be provided. For measuring feed flow rate accurately, a rotameter may be employed.

(ii)   Performance of a membrane is a strong function of operational conditions, viz. pressure, feed flow rate, and temperature. Therefore, the experiments may be carried out with varied operating conditions. This would allow one to check for the constancy of characteristics constants parameters of membranes, and suitability of transport models in numerical simulation.

(iii)   Other solute system, membranes, and RO devices should also be studied and tested in the experiemental unit.

(iv)   Development of membranes in the laboratory requires preparation under strict controlled conditions. Thus, more efforts are needed to arrive at conditions which may be employed to manufacture membranes with desired characteristics at large scale.

REFERENCES

1. A. Bottino et. al, Surface characterization of ceramic membrane by atomic force microscopy, Journal of Membrane Science, 95 (1994), pp. 289-296.

2. A.E.S. Al-zahrani et. al, An approximate analytical solution for the performance of reverse osmosis plants, Desalination, 75 (1989), pp. 15-24.

3. Alan S.Michaels, Membranes processess and their applications: needs; Unsolved problems and challenges of the 1990's, Desalination, 77(1990), pp 5-4.

4. A.S. Bal and A.N. Naidya, Application of membrane technology in waste water management, Chemical Engineering World, Vol. No. 1 (Jan.98), pp. 163-168.

5. A. Walch, Preparation and structure of synthetic membranes, Desalination, 46 (1983), pp. 303-312.

6. B.A. Winfield, A study of the factors affecting the rate of fouling of reverse osmosis membranes treating secondary sewage effluents, Water Research, 13 (1979), pp. 565-569.

7. Benito J. Marinas and Robert E. Selleck, Reverse osmosis treatement of multicomponent electrolyte solutions, journal of Membrane Science, 72 (1992), pp. 211-229.

8. Bipin S. Parekh, Reverse Osmosis Technology, Application for high purity water production, Millipore Corporation, Bedford, Massachusetts, pp. 9-194.

9. B.M. Misra, Desalination and water reuse in India, Chemical Business (April 1999), pp. 109-112.

10. Charles A. Sorber, Virus rejection by the reverse osomosis, ultrafiltration processess, Water Research, 6 (1972), pp. 1377-1388.

11. Conserving and reusing water, Chemical Engineering, (April 1982), pp. 125-128.

12. C.S. Slater et.al, Modeling of small scale reverse osmosis systems, Desalination, 52 (1985), pp. 267-284.

13. Edward Fredkin and Roger Banks, Coputerized Instrumentation and control, for reverse osmosis systems, Desalination, 75 (1989), pp. 141-148.

14. Erkki Vuorii et. al, Removal of Nodularin from brackish water with reverse osmosis or vacuum distillation. Water Research Vol. 31, No. 11 (1997), pp. 2922-2924.

15. Georges Belfort, et.al, Membrane regeneration for wastewater reclamation using reverse osmosis, Water Research, 7 (1993), pp. 1447-1559.

16. Gooding, Chemical Engineering,
(Jan. 7, 1985), pp. 56-57.

17. Goruganthu H. Rao and Kamalesh K. Sirkar, Explicit Flux Expression in Tublar reverse osmosis Desalination, Desalination, 27 (1978), pp. 99-116.

18. Harri Niemi and Seppo Palosarri, Flowsheet simulation of ultrafiltration and reverse osmosis, Journal of Membrane Science 19 (1994), pp. 111-124.

19. Harri Niemi and Seppo Palosarri, Calculation of permeate flux and rejection in simulation of ultrafiltration and reverse osmosis processess, Journal of Membrane Science, 84 (1933), pp. 123-137.

20. H. Mehdizadeh and J.M. Dickson, Theoritical modification of the surface force-pore flow model for reverse osmosis transport, Journal of Membrane Science, 42 (1989), pp. 119-145.

21. H. Ohya et.al, Design of reverse osmosis process, Desalination, 63 (1987), pp. 119-133.

22. H. Stratmann et.al, Development of new membranes, Desalination, 35 (1980), pp. 39-58.

23. Jay Mately and the staff of Chemical Engineering, Fluid Movers, Pumps, Compressors, Fans, and Blowersm McGraw-Hill Publication Co., New York, (1979).

24. Jea-Hua and Chung-Sung Tan, Separation of ethanol from aqueous solution by a method incorporating supercritical CO_2 with reverse osmosis, Journal of Membrane Science, 81 (1993), pp. 273-285.

25. J.M.K. Timmer et.al, Transport of latic acid through reverse osmosis and nanofiltration membranes, Journal of Membrane Science, 85 (1993), pp. 205-216.

26. Kinzi Asaka, Dielectric propertic of Cellulose acetate reverse osmosis membrane in aqueous salt solutions, Journal of membrane science, 50 (1990), pp. 71-84.

27. Lingying Zheng, Reverse osmosis membrane research in China, Desalination 50 (1984), pp. 115-124.

28. L. Kastclan-kunst et.al, FT 30 membranes of characterized porosities is the reverse osmosis organics removal from aqueous solution.

29. Lynn. E. Applegate, Membrane separation processess, Chemical Engineering, (June 1984), pp. 64-89.

30. M. Cheryan et.al, Reverse osmosis of Milk with thin film composite membranes, Journal of Membrane Science, 48(1990), pp. 103-114.

31. Permionics, Perma Pilot Plant, Baroda (Manual).

32. Peter R. Keller, Membrane Technology and Industrial Separation Techniques, Noyes data Corporation, Park ridge, New Jersey (1996), pp. 3-16.

33. Robert J. Peterson, Composite reverse and nanofiltration membranes, Journal of Membrane Science, 83 (1993), pp. 81-150.

34. Robert Rautenbach and Ingo Janisch, Reverse osmosis for the separation of organics from aqueous solutions, Chemical Engineering Procass, 23 (1988), pp. 67-75.

35. R.N. Patra et.al, Water and effluent water treatment using reverse osmosis Desalination, 67 (1987), pp. 507-521.

36. Scott B. McCray et.al, Reverse osmosis cellulose acetate membrane, II. Dependance of transport properties on acetyl content, Journal of Membrane Science, 59(1991), pp. 317-330.

37. Takeshi Matsuura and S. Sourirajan, Studies on reverse osmosis for water pollution control, Water Research, 6 (1972), pp. 1073-1086.

38. Tokehiko Kataoka et.al, Permeation equation developed for predicin of membrane performance in pervaporation, vapor permeation and reverse osmosis based on the solution, diffusion model, Journal of Chemical Engg. of Japan, Vol. 24, No. 1 (1991), pp.326-332.

39. Thoms A. Clair et.al, Concentration of aquatic dissolved organic matter by reverse osmosis, Water Research, 25(1991), pp. 1033-1037.

40. Torleiv Bilstad, Nitrogen separation from domestic wastewater by reverse osmosis, Journal of Membrane Science, 102 (1990), pp. 93-102.

41. Vassilis Gekas, Terminology for pressure driven membranes operations, Desalination, 68 (1998), pp. 77-92.

42. Walter J. Weber, JR., Physicochemical Processes-For Water Quality Control, Wiely interscience, (1972), pp.

43. W. Push, Performance of RO membrane in corelation with membrane structure, Transport mechanism of matter and module design. Desalination 77 (1990), pp.35-54.

Calibration Curve for Salt concentration

$$y = 0.0641x - 0.0094$$
$$R^2 = 0.9957$$
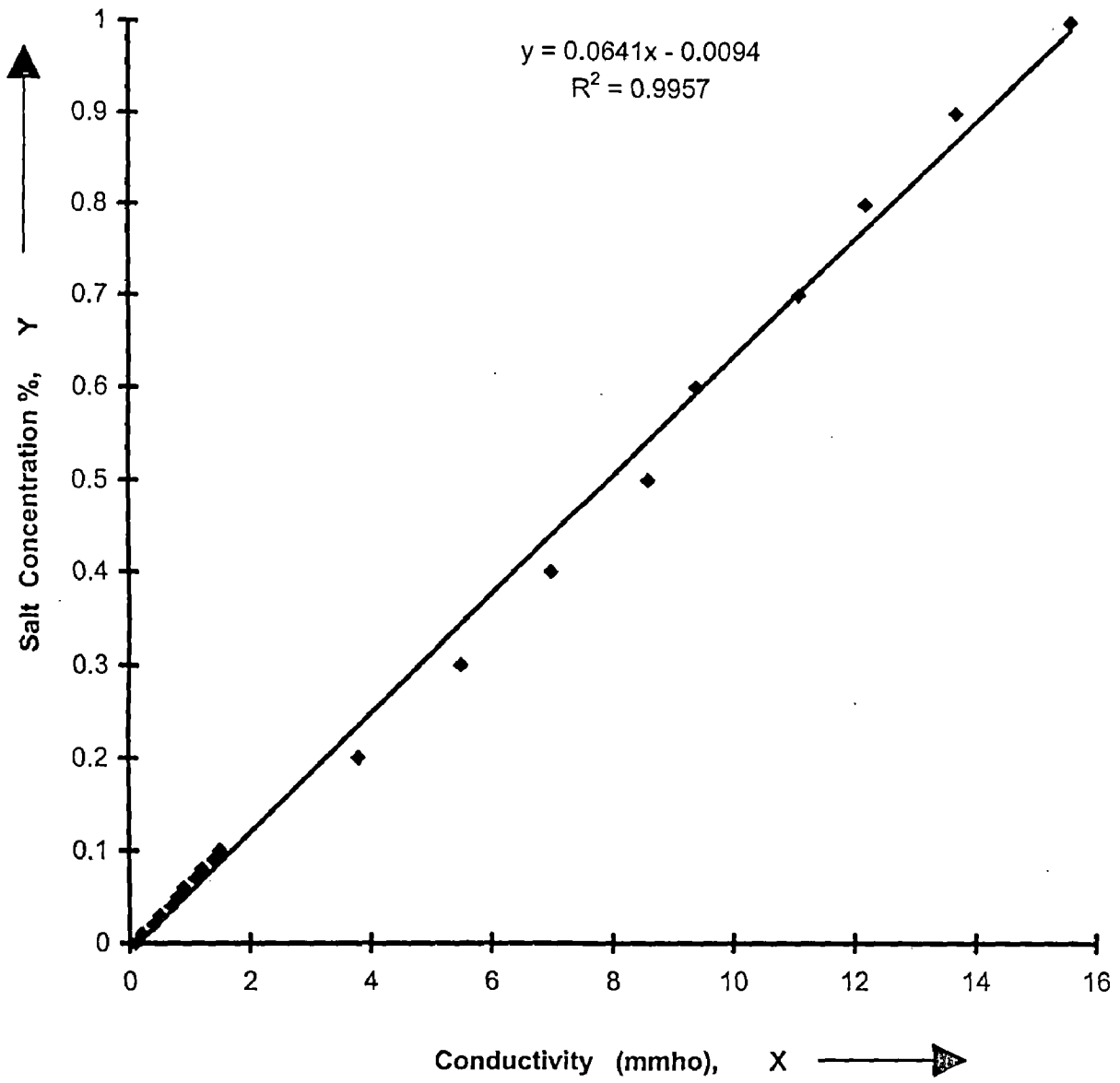
EXPERIMENTAL DATA FOR UNSTEADY-STATE MODE OF
OPERATION

Table B.1 Experimental data for initial feed concentration = 0.2%,
Initial feed volume = 19 litre, Feed flow rate = 14.063 l/min,
Pressure = $1.9*10^{19}$ kg/m*hr^2.

S.N	TIME min	PERMEATE CONCENTRATION kg/m^3	PERMEATE FLOW RATE ml/min	FEED CONCENTRATION kg/m^3	RETENTATE CONCENTRATION kg/m^3
1	0	0.02	832	2.20	2.34
2	5	0.09	800	2.70	2.86
3	10	0.09	800	3.40	3.63
4	15	0.15	736	4.70	4.92
5	20	0.34	720	7.20	7.30

Table   B.2 Experimental data for initial feed concentration = 0.4%,
Initial   feed   volume = 19 litre,   Feed   flow rate = 13.64 l/min,
Pressure = $1.9*10^{13}$ kg/m*hr^2 .

S.N	TIME min	PERMEATE CONCENTRATION kg/m^3	PERMEATE FLOW RATE ml/min	FEED CONCENTRATION kg/m^3	RETENTATE CONCENTRATION kg/m^3
1	0	0.15	708	4.20	4.47
2	5	0.15	656	5.05	5.24
3	10	0.28	628	6.21	6.46
4	15	0.28	600	7.88	8.14
5	20	0.54	424	10.2	10.26
6	25	0.79	360	12.58	12.45

Table   B.4 Experimental data for initial feed concentration = 0.8%,
Initial   feed   volume = 19litre, Feed flow   rate = 13.04 l/min,
Pressure = $1.9*10^{13}$ kg/m*hr^2.

S.N	TIME min	PERMEATE CONCENTRATION kg/m^3	PERMEATE FLOW RATE ml/min	FEED CONCENTRATION kg/m^3	RETENTATE CONCENTRATION kg/m^3
1	0	0.41	400	7.88	8.20
2	5	0.41	400	8.65	8.97
3	10	0.54	334	9.75	9.94
4	15	0.67	300	10.78	10.97
5	20	0.86	240	11.94	12.13
6	25	1.12	212	13.03	13.35
7	30	1.50	200	14.19	14.45
8	35	2.08	160	15.35	15.48

EXPERIMENTAL DATA FOR STEADY-STATE MODE OF
OPERATION, FOR THE CALCULATION OF SOLUTE
PERMEABILITY CONSTANT B_s

Table   C.1   Experimental data for initial feed concentration = 0.2%,
Initial feed   volume = 16 litre, Feed flow   rate = 13.95 l/min,
Pressure = $1.9*10^{13}$ kg/m*hr^2.

S.N	TIME min	PERMEATE CONCENTRATION kg/m^3	PERMEATE FLOW RATE ml/min	FEED CONCENTRATION kg/m^3	RETENTATE CONCENTRATION kg/m^3
1	0	0.15	848	2.02	2.21
2	5	0.15	922	1.89	2.08
3	10	0.15	878	2.02	2.21
4	15	0.15	886	1.89	1.02
5	20	0.08	898	1.83	2.02
6	25	0.15	930	1.83	1.95
7	30	0.15	886	1.83	1.95

Table C.2 Experimental data for initial feed concentration = 0.4%,
Initial feed volume = 16 litre, Feed flow rate = 13.79 l/min,
Pressure = $1.9*10^{13}$ kg/m*hr^2.

S.N	TIME min	PERMEATE CONCENTRATION kg/m^3	PERMEATE FLOW RATE ml/min	FEED CONCENTRATION kg/m^3	RETENTATE CONCENTRATION kg/m^3
1	0	0.34	712	4.21	4.47
2	5	0.27	748	4.21	4.53
3	10	0.22	724	4.21	4.69
4	15	0.22	740	4.27	4.59
5	20	0.22	760	4.27	4.65
6	25	0.15	800	4.40	4.72
7	30	0.22	832	4.34	4.85

Table C.3 Experimental data for initial feed concentration = 0.6%,
Initial feed volume = 16 litre, Feed flow rate = 13.95 l/min,
Pressure = $1.9*10^{13}$ kg/m*hr^2.

S.N	TIME min	PERMEATE CONCENTRATION kg/m^3	PERMEATE FLOW RATE ml/min	FEED CONCENTRATION kg/m^3	RETENTATE CONCENTRATION kg/m^3
1	0	0.45	620	5.64	5.89
2	5	0.33	628	5.70	5.95
3	10	0.39	650	5.77	6.08
4	15	0.39	628	5.86	6.14
5	20	0.39	686	5.86	6.20
6	25	0.39	650	5.89	6.27
7	30	0.39	652	5.89	6.33

Table C.4 Experimental data for initial feed concentration = 0.8%, Initial feed volume = 16 litre, Feed flow rate = 13.95 l/min, Pressure = $1.9*10^{13}$ kg/m*hr^2.

S.N	TIME min	PERMEATE CONCENTRATION kg/m^3	PERMEATE FLOW RATE ml/min	FEED CONCENTRATION kg/m^3	RETENTATE CONCENTRATION kg/m^3
1	0	0.46	522	7.58	7.58
2	5	0.39	540	7.70	7.70
3	10	0.39	522	7.83	7.83
4	15	0.39	534	7.95	7.95
5	20	0.39	600	8.08	8.08
6	25	0.39	600	8.20	8.20
7	30	0.33	600	8.27	8.27
8	35	0.39	600	7.95	14.2

Table C.5 Experimental data for initial feed concentration = 1.0%, Initial feed volume = 16 litre, Feed flow rate = 13.04 l/min, Pressure = $1.9*10^{13}$ kg/m*hr².

S.N	TIME min	PERMEATE CONCENTRATION kg/m³	PERMEATE FLOW RATE ml/min	FEED CONCENTRATION kg/m³	RETENTATE CONCENTRATION kg/m³
1	0	0.79	346	9.75	10.13
2	5	0.79	368	10.00	10.26
3	10	0.79	406	10.07	10.46
4	15	0.60	408	10.19	10.58
5	20	0.79	414	10.33	10.78
6	25	0.79	416	10.52	10.97
7	30	0.79	422	10.65	11.16
8	35	0.79	446	10.78	11.29

Table C.6 Experimental data for initial feed concentration =1.2%, Initial feed volume = 16 litre, Feed flow rate = 12.5 l/min, Pressure = $1.9*10^{13}$ kg/m*hr^2.

S.N	TIME min	PERMEATE CONCENTRATION kg/m^3	PERMEATE FLOW RATE ml/min	FEED CONCENTRATION kg/m^3	RETENTATE CONCENTRATION kg/m^3
1	0	0.99	328	11.42	11.74
2	5	0.85	330	11.49	11.87
3	10	0.99	288	11.68	12.00
4	15	0.99	276	11.80	12.13
5	20	0.99	312	11.87	12.13
6	25	0.99	312	12.07	12.45
7	30	0.99	312	12.00	12.45
8	35	0.99	336	12.13	12.58

EXPERIMENTAL DATA FOR THE CALCULATION OF OSMOTIC PRESSURE TO SOLUTE CONCENTRATION RATIO ψ AND SOLVENT PERMEABILITY CONSTANT A_W

Table D.1 Experimental data for initial feed concentration = 0.6%, Initial feed volume = 18 litre, Feed flow rate= 13 l/min.

S.N.	TIME min	PERMEATE FLOW RATE ml/min	PRESSURE kg/m*hr^2	PERMEATE CONCENTRATION kg/m^3	FEED CONCENTRATION kg/m^3
1	0	121.2	$1.14*10^{13}$	0.28	5.90
2	5	160.8	$1.27*10^{13}$	0.47	6.27
3	10	200	$1.39*10^{13}$	0.40	6.66
4	15	240	$1.53*10^{13}$	0.40	7.17
5	20	275.2	$1.65*10^{13}$	0.40	7.81
6	25	300	$1.78*10^{13}$	0.40	8.59
7	30	340	$1.98*10^{13}$	0.47	9.49

Table D.2 Experimental data for initial volume = 12 litre.

S.N.	TIME min	PRESSURE IN kg/m*hr^2	PRESSURE OUT kg/m*hr^2	PERMEATE FLOW RATE ml/min
1	0	$6.36*10^{12}$	$6.10*10^{12}$	400
2	5	$7.63*10^{12}$	$7.37*10^{12}$	500
3	10	$8.9*10^{12}$	$8.64*10^{12}$	520
4	15	$10.17*10^{12}$	$9.92*10^{12}$	600
5	20	$11.44*10^{12}$	$11.92*10^{12}$	700
6	25	$13.98*10^{12}$	$13.35*10^{12}$	860
7	30	$15.26*10^{12}$	$14.62*10^{12}$	10,00
8	35	$17.88*10^{12}$	$17.16*10^{12}$	11,60